Horizon 2020
Programme

GENIORS

Research and Innovation Action (RIA)

This project has received funding from the European Union's Horizon 2020 research and innovation programme under grant agreement No 755171.

Start date : 2017-06-01 Duration : 48 Months
http://geniors.eu/

GENIORS

Experimental and modeling studies of transfer kinetics in the reference separation processes

Authors : Pr. Simonin JEAN-PIERRE (CNRS), J.P. Simonin (CNRS-PHENIX), C. Boxall (ULANC), A. Lélias (CEA)

GENIORS - Contract Number: 755171

Project officer: Roger Garbil

Document title	Experimental and modeling studies of transfer kinetics in the reference separation processes
Author(s)	Pr. Simonin JEAN-PIERRE, J.P. Simonin (CNRS-PHENIX), C. Boxall (ULANC), A. Lélias (CEA)
Number of pages	60
Document type	Deliverable
Work Package	WP5
Document number	D5.1
Issued by	CNRS
Date of completion	2019-12-20 14:34:24
Dissemination level	Public

Summary

Three types of techniques have been used by the three partners to study the kinetics of extraction and stripping of various ions (Ce(III), Eu(III), Am(III), Fe(III) and Gd(III)) by the extractants TODGA, (cis)-mTDDGA and CyMe4-BTBP, sometimes in the presence of aqueous ligands such as SO3-Ph-BTP and PTD.

Approval

Date	By
2019-12-26 14:57:17	Pr. Christian EKBERG (Chalmers)
2020-01-06 13:17:22	Dr. Jean-Marc ADNET (CEA)
2020-04-22 09:14:35	Mr. Stéphane BOURG (CEA)

CONTENT

This project has received funding from the EURATOM research and training programme 2014-2018 under grant agreement No 755171. The content of this deliverable reflects only the author's view. The European Commission is not responsible for any use that may be made of the information it contains.

This project has received funding from the EURATOM research and training programme 2014-2018 under grant agreement No 755171. The content of this deliverable reflects only the author's view. The European Commission is not responsible for any use that may be made of the information it contains.

INTRODUCTION TO THE DELIVERABLE D5.1

EXPERIMENTAL AND MODELING STUDIES OF TRANSFER KINETICS IN THE REFERENCE SEPARATION PROCESSES

The aim of this preamble is to provide some preliminary information about the reports presented in this deliverable.

Three different partners have contributed to this deliverable: CEA, ULANC, and CNRS-PHENIX. These teams have used different techniques, namely a microfluidic device with parallel laminar flows (at CEA), a rotating diffusion cell (RDC, at ULANC), and a rotating membrane cell (RMC, at CNRS-PHENIX). See Figure 1.

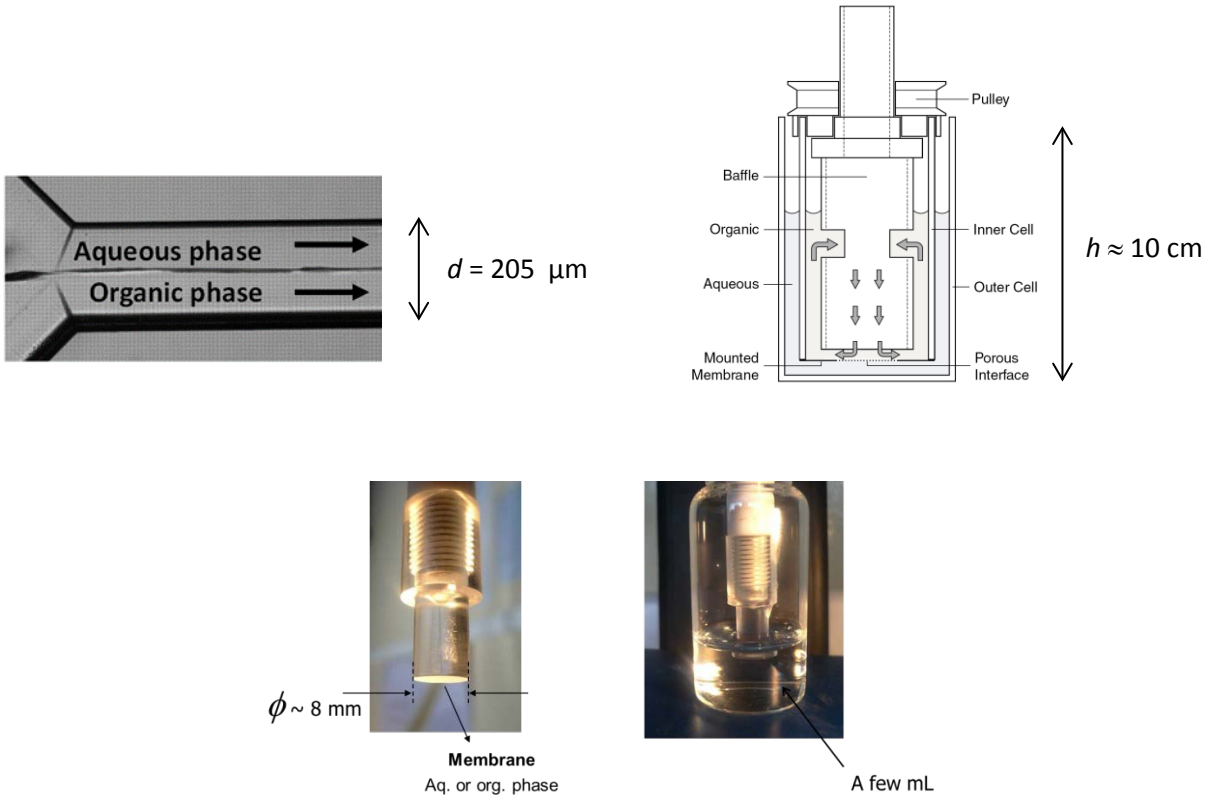

Figure 1: Microfluidic cell (top left), rotating diffusion cell (top right), and rotating membrane cell (bottom).

This project has received funding from the EURATOM research and training programme 2014-2018 under grant agreement No 755171. The content of this deliverable reflects only the author's view. The European Commission is not responsible for any use that may be made of the information it contains.

In a microfluidics experiment, 10 µL of each phase are continuously in contact in the Y-Y microchannel (of semi-circular cross-section, 1.25 cm long, 205 µm wide and 100 µm deep, corresponding to an inner volume of 20 µL). On the other hand, the entire experiment requires a total volume of ≈ 15 mL of solvent.

It might be worth mentioning some differences between the RMC and RDC techniques. They are as follows.

- The relative volumes of the phases are different in the two experiments.

In the RDC experiment, each phase on either side of the membrane is of relatively large volume: ≈ 75 mL and 35 mL for the aqueous and organic phases, respectively. The membrane has a thickness of 150 µm.

In the RMC, the membrane thickness is ≈ 60 µm or 100 µm, its diameter is 8 mm, its free volume is of a few microliters, and the volume of the external phase in the vial is of a few mL (usually 3 mL).

- The models used to describe the extracted rates are different.

CEA and CNRS-PHENIX assume that the reaction occurs strictly at the interface between the phases. Two interfacial kinetic rate constants are associated to this model: $k_{aq\rightarrow org}$ for the extraction rate constant, and $k_{org\rightarrow aq}$ for the stripping rate constant.

In contrast, ULANC assumes that the metal ion to be extracted first reacts with the extractant in a thin zone in the aqueous phase near the interface, in which the extractant is slightly soluble (see Figure 2). The so-formed complex is subsequently extracted into the organic phase. This model is sometimes called the mass transfer with chemical reaction (MTWCR) model. It was originally proposed by Carl Hanson[1-3]. A simplified version was devised later by Rod[4]. The latter model was based on the twin film model; it did not include any rotation-derived control of the thickness of the aqueous side diffusion layer. In the present report, the MTWCR model used by ULANC is inspired by the work of Rod; ULANC has adapted the Rod MTWCR model by adding Levich-derived control of the diffusion layer thickness.

This project has received funding from the EURATOM research and training programme 2014-2018 under grant agreement No 755171. The content of this deliverable reflects only the author's view. The European Commission is not responsible for any use that may be made of the information it contains.

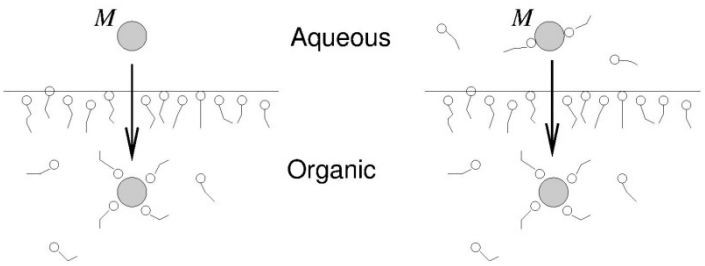

Figure 2: On the left hand-side, strictly interfacial complexation reaction of a metal ion M; on the right, MTWCR model in which the metal ion is first complexed by some extractant molecules in the aqueous phase (where the latter are slightly soluble), before being transferred to the organic phase after further complexation by other extractant molecules.

In the MTWCR model the parameters of the model are the transport of the extractant from the organic to aqueous phase, the rate of complexation of the metal with the ligand in the aqueous phase, the rate of decomplexation in the same phase, and the rate at which the complex diffuses back to the interface in order to be extracted.

Let us note finally that, in the kinetic experiments with the microfluidic cell and the RMC, the organic phase is previously pre-equilibrated with the aqueous phase; the aqueous phase was not pre-equilibrated when the diluent of the organic phase was TPH; it was pre-equilibrated when the diluent was octanol (so as to prevent a transfer of octanol to the aqueous phase during the experiments). No pre-equilibration of the phases was done in the experiments conducted by ULANC.

REFERENCES

1. C. Hanson, M. A. Hughes, and J. G. Marsland. *Proceedings of ISEC'74*, 2401, 1974.
2. R.J. Whewell, M. A. Hughes, and C. Hanson. *Proceedings of ISEC'77*, 185, 1979.
3. K. Kondo, S. Takahashi, T. Tsuneyuki, F. Nakashio. Solvent extraction of copper by benzoyl-acetone in a stirred transfer cell. *J. Chem. Eng. Jpn*, 11(3), 193-197, 1978.
4. V. Rod, Kinetics of Metal Extraction by Chelate Formation. Part I: Mass Transfer with a Fast Reversible Chemical Reaction and Product Extraction, *Chem. Eng. J.* 20 , 131 – 137, 1980.

This project has received funding from the EURATOM research and training programme 2014-2018 under grant agreement No 755171. The content of this deliverable reflects only the author's view. The European Commission is not responsible for any use that may be made of the information it contains.

STUDY OF EXTRACTION OF EUROPIUM(III), IRON(III) AND GADOLINIUM(III) BY (cis)- mTDDGA

CEA

A. Lélias, CEA Marcoule, DEN/DMRC/SPDS/LCPE, Bagnols s/ Cèze, France

1. INTRODUCTION

In the framework of the SACSESS project, CEA aimed to measure the global kinetics constants of ^{241}Am(III) and ^{152}Eu(III) ions from 0.2 M HNO_3 extracted by 0.2M TODGA-5% octanol diluted in TPH using the single drop technique. Involving a constant interfacial area (drops), this method based on the travel of a liquid drop (organic or aqueous phase) through a continuous phase required high volumes of solutions (500 mL for the continuous phase) and was not appropriate for this chemical system. Indeed ^{241}Am(III) and ^{152}Eu(III) extraction by the TODGA solvent is too high and fast at high nitric acidity to determine their kinetics constants in the extraction conditions: the acidity of the loaded solution had to be decreased from 3M to 0.2M [1]. Methods using smaller volumes and shorter contact times as the RMC or RDC are more adequate, as shown by Simonin and Boxall below.

Another way consists of the microfluidics technology that some authors use to study the mass transfer kinetics in the nuclear field [2, 7]. Enabling a shorter diffuse layer, microfluidics chips offer a well-controlled interfacial area and a significant decrease of contact times. In a recent paper [8], CEA describes an original experimental setup allowing acquisition of kinetic constants using high velocities in order to reduce dramatically the diffusion contribution on mass transfer kinetics, allowing a better understanding of the phenomena governing the mass transport.

Thanks to the European partner, kinetics data on Am, Eu, Ln have already been studied with TODGA based solvents [1, this work]. We then propose to use this microfluidics method on an extracting system developed in the GENIORS program by the Twente University in collaboration with Jülich and KIT: mTDDGA 0.2 M in TPH. The choice of this extracting system relies on the proposal of future irradiation loop tests [9] with a loaded solution of Ln(III), Fe(III) in HNO_3 3M extracted by mTDDGA and back-extracted by PTD. Thermodynamic data have already been acquired within these systems [10-11] but no kinetics study has been yet carried out.

This project has received funding from the EURATOM research and training programme 2014-2018 under grant agreement No 755171. The content of this deliverable reflects only the author's view. The European Commission is not responsible for any use that may be made of the information it contains.

2. EXPERIMENTAL

1. SETUP

To study the kinetic constant, stratified flow has been chosen. The mass transfer in this flow configuration can be limited by the molecular diffusion when the interfacial mass reaction is faster. Nevertheless, the use of high velocities flow aims to reduce both aqueous and organic diffusive films thickness, where the molecular diffusion usually occurs. We then assume that such a concept will allow a better description of the mass transfer contribution to the global kinetic of the extraction process.

A schematic diagram of the experimental bench is shown in Fig 1. A Y-Y geometry glass microchip from Dolomite® (Part number 3200008) is used. The Y-Y microchannel was 1.25 cm long, 205 µm wide and 100 µm deep with a semi-circular cross-sectional area (Fig. 2). Inlet feeders are equipped with stainless steel filters (10 µm porous) to prevent any intake of pollutants in the microfluidic chip. Two Coriolis flowmeters (Bronkhorst ML120) allow the measure of the inlet flowrates. Flowrates are controlled by a Fluigent MFCS - EX pressure pump connected to inlet vessels (100 mL glass vials) and to exits. The aqueous stream is collected into a 100 mL glass vial while a T solenoid valve (Fluigent 2 – SWITCH) allows selecting an organic outlet (100 mL vial for waste or a 2 mL vial for sampling operations). A Zeiss AX10 standard optical microscope is used to observe the flows.

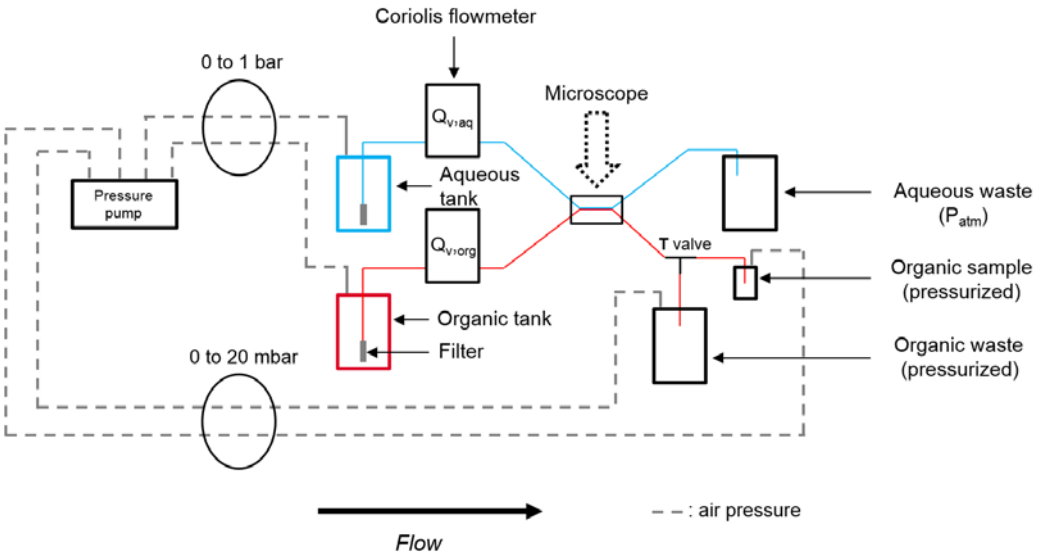

Figure 1: Experimental setup

This project has received funding from the EURATOM research and training programme 2014-2018 under grant agreement No 755171. The content of this deliverable reflects only the author's view. The European Commission is not responsible for any use that may be made of the information it contains.

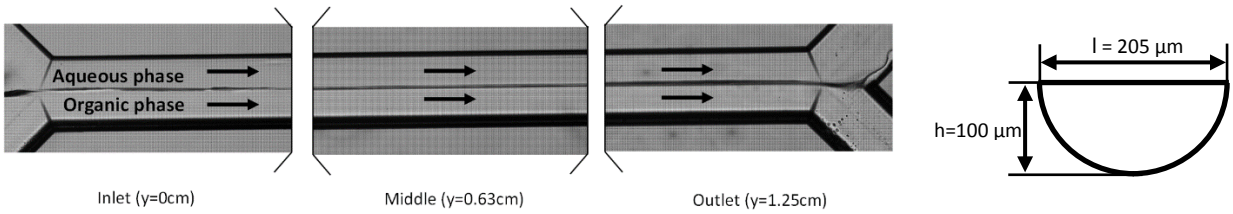

Figure 2 : Y-Y dolomite chip used in this study

OPERATING PROCEDURES

All experiments are realized as follows: the flow rates are set by using the accurate entrance pressure to ensure a 50/50 phase proportion inside the microchannel and ease separation at the outlet. Moreover, the symmetrical shape of the microchip also eases the phase separation even at high flow velocities. During experiments, the aqueous stream is collected into a unique vessel while the solvent is sampled. Studying the extraction step, contamination of the organic phase by the other one has to be avoided. Thus, a thin layer of the solvent is sent to the aqueous exit thanks to a compensation pressure at the aqueous outlets. With this method, the organic phase is pure and ready for analysis. In the present experimental conditions, different inlet pressures are applied from 300 to 900 mbar, compensation pressure ranges from 0 to 5 mbar. The data acquisitions are carried out at hydrodynamic steady state.

2. PREPARATION OF THE FEEDS AND ANALYSIS

TPH was purchased from NOVASEP. (cis)-mTDDGA was synthesized by the Laboratory of Molecular Nanofabrication from Twente university with 99% purity. Before carrying out any experiment, the 0.5 M mTDDGA/TPH solvent was pre-treated by contacting it with a 3 M HNO_3 solution (A/O = 3). The acidic solution was prepared by dissolving inactive Eu, Gd and Fe nitrate salts in HNO_3 3M in order to get a 10^{-2} M concentration, that was then diluted in HNO_3 3M to get a cation concentration of 10^{-3} M. The composition of the solutions is summarized in Table 1.

Table 1: Characterization of the feeds – n.d. = not determined

	[HNO_3] (M)	[Eu] (mol.L^{-1}) *(g.L^{-1})*	[Fe] (mol.L^{-1}) *(g.L^{-1})*	[Gd] (mol.L^{-1}) *(g.L^{-1})*	Density (g.cm^{-3}) 25°C	Dynamic viscosity (mPa.s) – 24°C
Aqueous feed	3.1	0.010 *0.153*	0.010 *0.057*	0.010 *0.161*	1.1071	1.030
Solvent	n.d.				0.8320	10.55

The phase viscosities are determined by a RheoSense microVISC. The phase densities are measured by the Bronkhorst ML120 flowmeters and randomly double-checked by a density meter (Anton Paar DMA 5000). The acidities of each phases are measured by

This project has received funding from the EURATOM research and training programme 2014-2018 under grant agreement No 755171. The content of this deliverable reflects only the author's view. The European Commission is not responsible for any use that may be made of the information it contains.

potentiometers (Metrohm Titrando). The aqueous cations concentrations are determined by ICP-AES (Perkin-Elmer OPTIMA 8300DV). The analysis of the extracted cations requires their stripping using a mixture of 0.2 M TEDGA (Pharmasynthese) + 0.5 M oxalic acid in deionized water. One volume of the organic phase is contacted with three volumes of this stripping solution during 30 minutes at 25°C. If necessary, this aqueous phase is further diluted. Uncertainty on element concentrations determined by ICP-AES is ± 10%.

3. KINETICS EXPERIMENTS

Faced to the impossibility to performed the experiments with spiked solutions, the experimental bench being into a non-nuclear laboratory, a first aqueous feed containing Eu(III), Fe(III) and Gd(III) at 10^{-4} M (over 10^{-3} $g.L^{-1}$) at HNO_3 3M was prepared. We assumed that the obtained solutions would be high enough to be analyzed. Experiment was carried out at 25°C. Unfortunately, the cations concentrations in the organic samples were too low to be detected by ICP.

The following extraction experiment of Eu(III), Fe(III) and Gd(III) was carried out at HNO_3 3M with a concentration of cations at 10^{-3} M (over 10^{-2} $g.L^{-1}$, see Table 1) with the 0.5M (cis)-mTDDGA/TPH solvent at 25°C. 3 inlet pressures were applied, around 400 mbar, 500 and 700 mbar. A point at 900 mbar was attempted but interfacial instabilities did not allowed getting a pure solvent sample. In order to keep a 50/50 phase proportion inside the microchannel, the ratio between the flow velocities (O/A) has to be around 0.16.

The cations concentrations could be measured but remain very low and the extraction yields don't exceed 0.24 % (Table 2) while the Eu, Gd and Fe distribution ratios are high like those determined in spiked conditions [10-11]. As reported in Table 3, they are even so higher for Eu and Gd than literature ones.

Table 2: Characterization of the organic samples at various pressure. The extraction yield is calculated according to Eq. 1

P_{org} (mbar)	[Eu] ($mol.L^{-1}$)	[Eu] ($g.L^{-1}$)	[Fe] ($mol.L^{-1}$)	[Fe] ($g.L^{-1}$)	[Gd] ($mol.L^{-1}$)	[Gd] ($g.L^{-1}$)	Inlet Density ($g.cm^{-3}$) 25°C
470	4.4×10^{-6}	6.6×10^{-4}	1.7×10^{-5}	9.5×10^{-4}	5.4×10^{-6}	8.4×10^{-4}	0.832
590	4.4×10^{-6}	6.7×10^{-4}	2.6×10^{-5}	1.5×10^{-3}	5.2×10^{-6}	8.1×10^{-4}	
770	4.4×10^{-6}	6.7×10^{-4}	1.2×10^{-5}	6.6×10^{-4}	5.2×10^{-6}	8.3×10^{-4}	
Max. extraction yield (%)	0.07		0.15		0.24		

This project has received funding from the EURATOM research and training programme 2014-2018 under grant agreement No 755171. The content of this deliverable reflects only the author's view. The European Commission is not responsible for any use that may be made of the information it contains.

$$Extraction\ Yield = \frac{[M]_{org,out}}{[M]_{initial}} * \frac{Q_{org}}{Q_{aq}} \quad (1)$$

Table 3: Distribution ratios of Eu(III), Fe(III) and Gd(III) at 10^{-3} M in HNO_3 3 M extracted by 0.5 M (cis) m-TDDGA /TPH

	HNO_3	Eu(III)	Fe(III)	Gd(III)
Lit. data [10-11]	3.6	265	(1.0 at 2M HNO_3)	177
This work	3.1	431.2	1.0	399.5

The very short residence times of both the phases can explain these results. Despite the viscosity difference, the aqueous and organic feeds move *a minima* between 0.5 and 0.08 $m.s^{-1}$ respectively corresponding to a residence time from 24 to 151 ms respectively (Table 4). When increasing the pressure, velocity increases and residence times decreases logically. We can then assume that the extraction kinetics is not fast enough to be observed at this time scale. Slowing down the residence times of the both phases have then to be investigated.

Table 4: Hydrodynamic characteristics of the feeds during the extraction of Eu(III), Fe(III) and Gd(III) at 10^{-3} M in HNO_3 3 M by 0.5 M (cis) m-TDDGA /TPH

Q_{aq} ($m^3.s^{-1}$)	Q_{org} ($m^3.s^{-1}$)	u_{aq} ($m.s^{-1}$)	u_{org} ($m.s^{-1}$)	t_{aq} (s)	t_{org} (s)
4.2E-09	6.6E-10	0.500	0.078	0.024	0.151
5.5E-09	8.8E-10	0.650	0.104	0.018	0.113
8.0E-09	1.2E-09	0.944	0.137	0.012	0.086

Another point to mention is the existence of the thin part of the organic layer sent into the aqueous phase. In the present study, it represents 10% of the aqueous channel as depicted in Fig.3. This method avoids the contamination of the solvent, but as demonstrated in literature [7], if the organic phase is not perfectly homogenized this layer could deplete the solvent of a certain amount of cations and have repercussions on the cations measurements. Considering the cations concentration measured, the major part of the Eu(III), Fe(III) and Gd(III) extracted is supposed to be in the thin organic stream sent to the aqueous outlet. To confirm this hypothesis, new experiments have to be carried out with higher cations concentration (1, 10 and 20 $g.L^{-1}$).

This project has received funding from the EURATOM research and training programme 2014-2018 under grant agreement No 755171. The content of this deliverable reflects only the author's view. The European Commission is not responsible for any use that may be made of the information it contains.

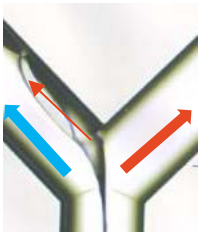

Figure 3: Outlet of the Y-Y chip. Links, the aqueous channel. Right, the organic channel. In red Eu, Fe, Gd in (cis)-mTDDGA 0.5 M/ TPH. In blue, Eu, Fe, Gd 10^{-3} M in HNO_3 3 M

3. MASS TRANSFER

The global mass transfer constant is established by plotting the organic cation concentration, C_{org}, *vs*. residence time. Assuming a first order reaction, the mass balance of the extraction reaction leads to Eq. 2,

$$Ln\left(1-\frac{C_{org}}{C_{org}^{*}}\right)=-\frac{A}{V}K_g\,t \qquad (2)$$

Where C_{org} = organic concentration [M], C_{org}^{*} = interfacial organic concentration [M], A = interfacial area [mm^2], V = volume of each phase [mm^3], D = distribution coefficient with $D=\frac{K_{aq}}{K_{org}}=\frac{C_{org}^{*}}{C_{aq}^{eq}}=\frac{C_{org}^{eq}}{C_{aq}^{*}}$. All parameters are known except K_g [$m.s^{-1}$], the global mass transfer constant for the organic phase.

As shown in Table 2, there are some discrepancies between cations concentration values. While they have to decrease when the residence times shorten, Eu(III) remains stable and Fe(III) like Gd(III) concentration change randomly. The low values are in question. Thus, the global mass transfer constants of each cation can only be estimated: K_g is approximatively 10^{-9} $m.s^{-1}$ for Eu(III) and Gd(III) and quite faster for Fe(III) with 10^{-5} $m.s^{-1}$ (Fig.4). Considering the poor and random concentrations measured, a discussion of these results seems unnecessary. However, if focusing on Eq. 2 and considering a quantitative mass transfer, the global mass transfer kinetics constants cannot exceed 10^{-5} $m.s^{-1}$ for lanthanides due to the high distribution ratio of these elements in our experimental conditions. On the contrary, the low D of Fe(III) leads to estimate its K_g around 10^{-3} $m.s^{-1}$.

This project has received funding from the EURATOM research and training programme 2014-2018 under grant agreement No 755171. The content of this deliverable reflects only the author's view. The European Commission is not responsible for any use that may be made of the information it contains.

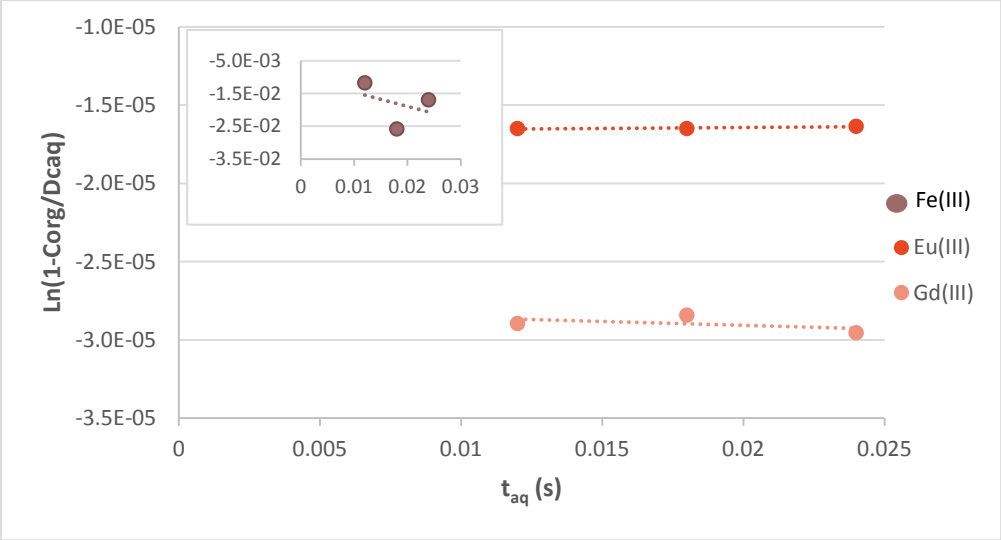

Figure 4: Influence of the aqueous residence time on the concentration of the extracted cations. Eu(III), Fe(III), Gd(III) 10^{-3} M in HNO_3 3 M extracted by (cis)-mTDDGA 0.5 M/ TPH, 25°C.

4. CONCLUSION AND FURTHER WORK

These first results indicate that the microfluidics setup used to determine the mass transfer kinetics constants of Eu(III), Fe(III) and Gd(III) has to be improved. Concentration of the extracted cations is too low to be accurately exploited. Two reasons can be put forward: whether the major part of the extracted cations is in the thin layer sent into the aqueous phase, whether the extraction kinetics is to slow to occur at the range of the studied residence times.

In any case, an extrapolation of a quantitative extraction in the considered conditions leads to conclude that the mass transfer kinetics constants of Eu(III) and Gd(III) are around 10^{-5} $m.s^{-1}$ and 10^{-3} $m.s^{-1}$ for Fe(III). Compared to the results of Simonin with RMC for Eu(III) extracted by TODGA (5% octanol), this value is of the same order of magnitude. Fe(III) seems to be quite high and has to be confirmed.

To support these assumptions, new experiments are envisioned:

- Extraction of the Eu(III), Fe(III) and Gd(III) at higher cations concentration (1, 10 and 20 $g.L^{-1}$) in order to ensure the influence of the thin layer sent into the organic phase on the mass transfer;
- Carrying out experiments with slower velocities;

This project has received funding from the EURATOM research and training programme 2014-2018 under grant agreement No 755171. The content of this deliverable reflects only the author's view. The European Commission is not responsible for any use that may be made of the information it contains.

- Carrying out the extraction of Eu(III) in HNO_3 3M with TODGA 0.2 M (5% octanol) to compare the results with the RMC, RDC and single drop technics;
- If authorized, to investigate within the microfluidics device the mass transfer of ^{152}Eu, ^{241}Am and ^{57}Fe by the mTDDGA solvent. The analytic difficulties will be avoided. If not allowed, data acquisition in glove box could be envisioned with the Single Drop technic in aqueous phase configuration.

Finally, this work has to be complete by the study of the stripping kinetics using PTD kindly provided by POLIMI.

REFERENCES

[1] J.-P. Simonin, C. Boxall, A. Lélias 2015, SACSESS delivrable D12.5

[2] H. Hotokezaka, *Prog. Nucl. Energy* 2005, 47 (1), 439-447. DOI: 10.1016/j.pnucene.2005.05.045.

[3] K. P. Nichols, *J. Am. Chem. Soc* Chemical Society 2011, 133 (39), 15721-15729. DOI: 10.1021/ja206020u.

[4] M. Yamamoto, *J. Sep. Sci.* 2015, 38 (10), 1807-1812. DOI: 10.1002/jssc.201401315.

[5] C. A. Launiere, *Ind Eng Chem Res* 2016, 55 (7), 2272-2276. DOI: 10.1021/acs.iecr.5b04691.

[6] Q. Li, *Chem. Eng. Sci.* 2016, 143, 276-286. DOI: 10.1016/j.ces.2016.01.004.

[7] G. L. Nelson, *Anal. Chem.* 2018, 90 (14), 8345-8353. DOI: 10.1021/acs.analchem.7b04330.

[8] F. Corne, A. Lélias , A. Magnaldo, C. Sorel, N. Di Miceli Raimondi, L. Prat *Chem. Eng. Technol.* 2019, 42, 2223-2230. DOI: 10.1002/ceat.201900111

[9] Geniors Meeting, DM2 presentation, Madrid 2019 June 18-19

[10] Geniors Meeting, SCK-CEN / Jülich presentation, Madrid 2019 June 18-19

[11] R. Malmbeck, D. Magnusson, A. Geist, *J. Radioanl. Nucl. Chem.* 2017, 314, 2531-2538. DOI: 10.1007/s10967-017-5614-2.

This project has received funding from the EURATOM research and training programme 2014-2018 under grant agreement No 755171. The content of this deliverable reflects only the author's view. The European Commission is not responsible for any use that may be made of the information it contains.

KINETIC STUDIES OF EXTRACTIONS USING TODGA: INSIGHTS FROM EXPERIMENTAL AND MODELLING STUDIES OF LN(III) EXTRACTIONS

ULANC

A. Jackson, C. Boxall, M. Bromley, Engineering Department, Lancaster University, Lancaster LA1 4YR, UK,

R. Taylor, D. Woodhead, Central Laboratory, The UK National Nuclear Laboratory, Sellafield, Seascale, Cumbria CA20 1PG, UK

1. INTRODUCTION

The kinetics of liquid/liquid extraction processes play a major role in determining key process features during scale-up such as choices of contactor, extractant, reagents, flow rates, temperature etc. In turn, selected plant & process parameters strongly influence process and radiological safety through e.g. sensitivity to maloperations. Safe operations, including a predictive capacity for the definition of the safe operating envelope and sensitivity analysis of the limits of that envelope to variations in key process parameters, are therefore underpinned by a robust understanding of liquid/liquid extraction kinetics. This understanding requires separate experimental measurement of both mass and interfacial transfer kinetics.

Commonly used plants in nuclear separations include, in order of decreasing residence time and increasing rates of convective-diffusive mass transfer, mixer-settlers, pulsed columns and centrifugal contactors. The ability to comprehensively interrogate liquid/liquid transfer kinetics for candidate separations processes and platforms therefore requires a range of techniques that encompass both representative mass transfer time domains (shear rates) and geometries for those platforms.

As part of a GENIORS matching PhD studentship funded by the UK EPSRC and the National Nuclear Laboratory, the kinetics of extraction for the following system has been studied at Lancaster University using a Rotating Diffusion Cell (RDC):

- Lanthanide (III) ions by TODGA

The RDC covers mass transfer time domains characteristic of centrifugal contactors, providing interfacial kinetic information, mechanistic insights and rates of metal-ligand complexation and decomplexation. Since its commencement in October 2017, work during the PhD has followed parallel modelling and experimental tracks, with this report then

This project has received funding from the EURATOM research and training programme 2014-2018 under grant agreement No 755171. The content of this deliverable reflects only the author's view. The European Commission is not responsible for any use that may be made of the information it contains.

presenting a summary of progress during the first two years of the student's registration period. The report is divided into six sections.

- The first section describes the RDC technique and presents an exemplar data recorded during study of the extraction of Ce(III) from nitric acid by TODGA using non-pre-contacted aqueous and organic phases.
- The second section discusses and explains a surprising feature of this data: that the rate of extraction abruptly slows at long extraction times.
- The third section presents a first version semi-analytical model of the extraction rate data recorded at extraction times prior to the abrupt slowing in extraction rate mentioned above.
- Driven by the results of the semi-analytical modelling above, the fourth section describes an exploratory MALDI-TOF mass spectrometry study of the solubility of TODGA in aqueous solutions of nitric acid.
- The fifth section presents a revised version of the model presented in section 3 of this report wherein the governing convection-diffusion equations are solved numerically rather than semi-analytically. This approach allows for some of the assumptions necessary for analytical solution to be relaxed, resulting in a substantially better fit between modelled and experimental data.
- Finally, the sixth section describes some preliminary extraction data recorded in preparation for RDC studies of the extraction of neodymium (III) from nitric acid solutions by TODGA.

2. THE ROTATING DIFFUSION CELL AND ITS USE IN THE STUDY OF CE(III) EXTRACTION BY TODGA

The rotating diffusion cell (RDC) allows for the study of coupled interfacial mass transfer of liquid/liquid extraction processes used by the nuclear industry. The process of interest for this report is the i-SANEX process in which trivalent actinides and lanthanides (such as Am and Cm), present in a PUREX raffinate, are selectively extracted into an organic phase containing TODGA; a ligand that complexes with the trivalent metal ions.

The RDC is derived from the Lewis Cell but comprises two separate compartments into which the two solution phases are contained. Figure 1 shows a schematic cross section of the RDC. In the embodiment used in the experiments described in this report, it is comprised of an inner rotating cylinder, containing the organic solution phase, and an outer non-

This project has received funding from the EURATOM research and training programme 2014-2018 under grant agreement No 755171. The content of this deliverable reflects only the author's view. The European Commission is not responsible for any use that may be made of the information it contains.

rotating reaction vessel, containing the aqueous solution phase. These are separated by a porous membrane filter mounted at the lower open end of the inner cylinder.

The mounted nitrocellulose membrane (Millipore GSWP04700, 0.22 µm pore size, 150 µm thickness) is treated with clearing solvent (33.3% n-hexane, 33.3% 1,2-dichloroethane, 33.3% 1,4-dioxane) to selectively collapse the porosity around the membrane perimeter while preserving a central porous disc. This disc, which must be positioned within the controlled flow region at the center of the cylinder (see below), then provides an interface of defined area between the two solution phases, across which the transport of species can be studied.

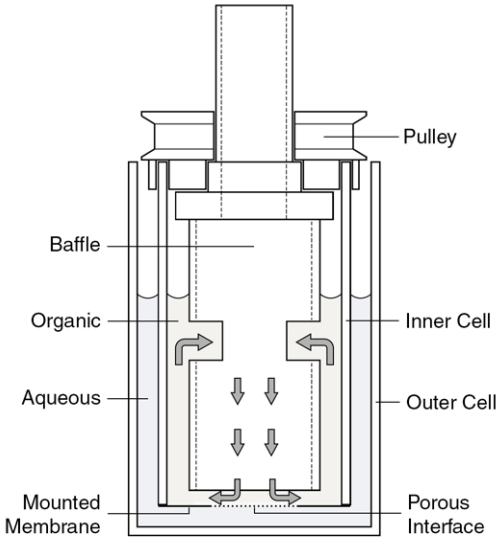

Figure 5: Rotating Diffusion Cell

Rotation of the inner cylinder of the RDC generates hydrodynamic flow at each side of the interface membrane. At the outer membrane surface, this rotation generates desirable hydrodynamics which match those of widely studied rotating disc systems without modification. The solution in the inner cylinder is subjected to significant centrifugal force during cell rotation. Consequently, a PTFE baffle must be employed to regulate the hydrodynamic flow inside the cylinder and generate a flow pattern towards and normal to the interface. Centrifugal force causes the solution to exit the baffle via a 2 mm gap above the interface, generating rotating disc-like hydrodynamics across the inner membrane surface as well.

By establishing this hydrodynamic environment at each side of the solution phase interface, the RDC enables the monitoring of both physical and chemical kinetics based on kinetic selectivity, through a high sheer, low residence environment, thermodynamic selectivity, through a low sheer, high residence environment, and the transition between the two regimes.

This project has received funding from the EURATOM research and training programme 2014-2018 under grant agreement No 755171. The content of this deliverable reflects only the author's view. The European Commission is not responsible for any use that may be made of the information it contains.

In the RDC experiments described in this, the organic phase consists of 0.2 mol.dm^{-3} TODGA in n-dodecane (5% octanol) and the aqueous phase consists of 10 mmol.dm^{-3} Ce(III) metal ions in 1.0 mol.dm^{-3} HNO_3, simulating a PUREX raffinate. The transfer of Ce(III) into the organic phase, via a ligand/metal ion complexation process, is measured using UV-visible spectrophotometry, its peak absorbance at 346 nm being converted into concentration of organic Ce(III) using its extinction coefficient at this wavelength of 0.0092 m^3 mol^{-1} cm^{-1}.

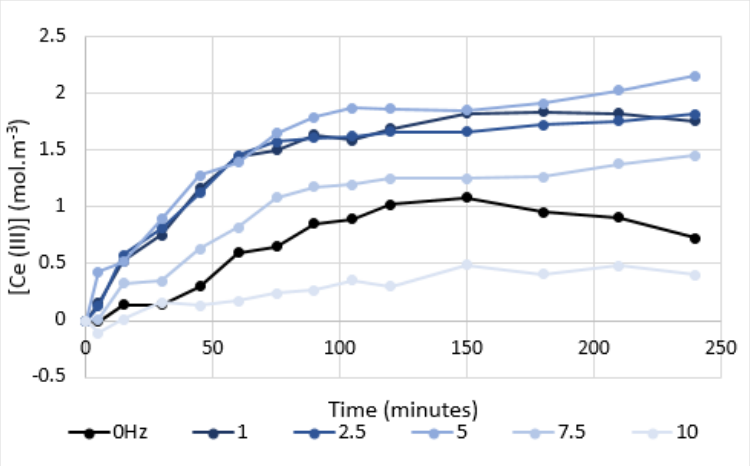

Figure 6: Ce(III) concentration with time in RDC organic phase at rotation speeds (0-10Hz) (Bromley, 2015).

Figure 2 shows exemplar RDC data recorded for the extraction of Ce(III) from nitric acid by TODGA. Specifically, Figure 2 shows the concentration of Ce(III) measured in the organic phase in the inner cylinder as a function of extraction time at a range of inner cylinder rotation speeds. The data shows two distinct regions. Before extraction times of 60 to 100 minutes, the extraction takes place at a relatively constant rate at each rotation speed. However, after extraction times of approximately 60 to 100 minutes, the extraction rate abruptly decreases and appears to plateau.

We will first discuss the origin of this latter, long extraction time behaviour before moving on to a detailed discussion of the rotation speed dependence of the extraction rate at short extraction times of less than 60 minutes.

This project has received funding from the EURATOM research and training programme 2014-2018 under grant agreement No 755171. The content of this deliverable reflects only the author's view. The European Commission is not responsible for any use that may be made of the information it contains.

3. CE(III) EXTRACTION BY TODGA – ORIGIN OF THE EXTRACTION RATE PLATEAU AT LONG EXTRACTION TIMES.

Results of Ce(III)-TODGA extraction studies conducted using the RDC during SACSESS indicate:

(i) that the key metal-ligand complexation reaction occurs within the aqueous phase, with the resultant complex then undergoing phase transfer into the solvent phase (to be discussed in more detail in section 3 below);

(ii) that, within any one RDC experiment conducted using a fresh solution of TODGA in dodecane that has NOT been pre-contacted with nitric acid, the rate of cerium extraction by TODGA decreases with increasing experiment run time – as discussed in reference to Figure 2 above and further and more plainly evidenced in the excerpted data of Figure 3 below;

(iii) that HNO_3 is co-extracted with cerium (III) and that, within any one RDC experiment conducted using a fresh solution of TODGA in dodecane that has NOT been pre-contacted with nitric acid, the rate of HNO_3 extraction by TODGA appears to be constant with increasing experiment run time – again see Figure 3.

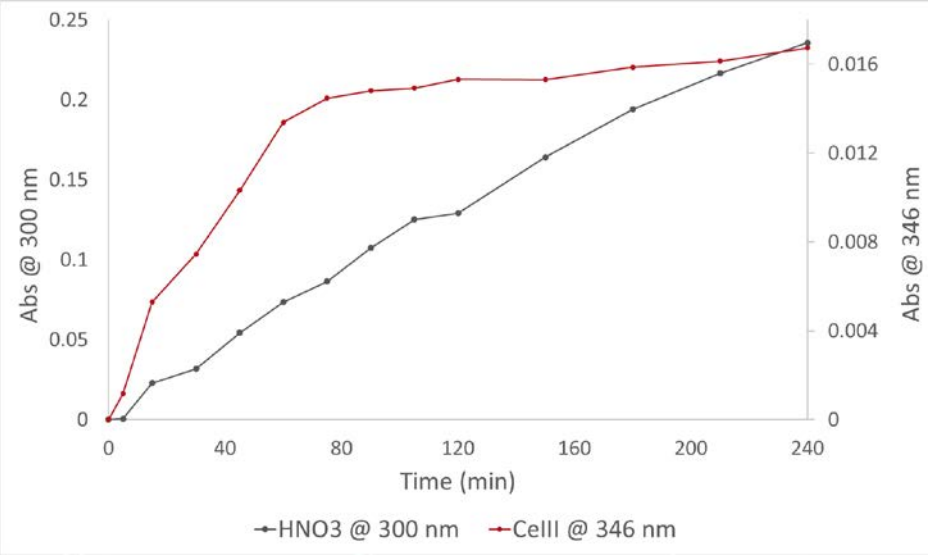

Figure 3. Amount of Ce(III) and HNO_3 extracted from aqueous phase to the TODGA organic phase as a function of time in an RDC experiment. Extracted Ce(III) determined by measurement of the Ce(III)-TODGA complex peak absorbance at 346 nm (red series). Extracted HNO_3 determined by measurement of the HNO_3-TODGA complex peak absorbance at 303 nm (black series). Absorbance vs time plots recorded at an RDC rotation rate of 2.5 Hz. Inner cylinder phase comprised of 0.2 mol dm^{-3} TODGA in 5% octanol in dodecane. Outer vessel phase initially comprised of 10 mmol dm^{-3} Ce(III) in 1 mol dm^{-3} HNO_3.

This project has received funding from the EURATOM research and training programme 2014-2018 under grant agreement No 755171. The content of this deliverable reflects only the author's view. The European Commission is not responsible for any use that may be made of the information it contains.

The effect described in point (ii) has been attributed to effects resulting from an increase in organic phase acidity with time, arising from the extraction by TODGA of HNO_3 (simultaneous with the desired extraction of Ce(III)) from the aqueous phase into organic phase as any one RDC experiment progresses – the effect described in point (iii) above. This conclusion is supported by the fact that the Ce(III) extraction rates observed using TODGA solutions that HAVE been pre-contacted with aqueous HNO_3 are substantially lower than those observed when using TODGA solutions that have NOT been pre-contacted.

An investigation into the influence of HNO_3 on TODGA in dodecane solutions conducted between SACSESS and GENIORS revealed an increase in organic phase viscosity with increasing organic phase acidity, suggesting HNO_3-driven aggregation of the TODGA into reverse micelles. Such aggregation may be inhibitive of the transition of the extractant molecule into the aqueous phase where complexation has been shown to take place, thus reducing the rate of fission product extraction. Aggregation of TODGA to form reverse micelles has been studied by a range of authors including Nave et al (2004), Jensen et al (2007), Ganguly et al (2011) and Gray et al using techniques such as SAXS, SANS, tensiometry, dynamic light scattering and viscometry. The main finding of these studies of relevance to this report is that solutions of TODGA of similar composition to that used in the work reported here exhibit reverse micelle formation when contacted and equilibrated with solution of nitric acid solutions wherein the HNO_3 concentration is ~0.7 mol dm^{-3} or greater.

Based on this finding, the work described in this report period has focussed on correlating the putative HNO_3-triggered reverse micellation event observed in our dynamic extraction RDC studies with the above-described equilibrium studies of TODGA aggregation in the presence of HNO_3 published by Nave, Jensen, Ganguly and Gray and their co-authors.

Specifically, we have reviewed and revisited data from Nave et al, FZJ, KIT and NNL describing the equilibrium extraction of HNO_3 into solutions of TODGA in TPH, dodecane, Exxsol D80 – both in the presence and absence of octanol. We have then used this data to derive polynomials relating the concentration of HNO_3 extracted into the TODGA phase to the concentration of nitric acid in the aqueous phase from which the HNO_3 has been extracted, see Figure 4 below.

We have conducted our own equilibrium studies of the extraction of HNO_3 from aqueous solution into solutions of 5% octanol in dodecane – and thence used UV-visible adsorption spectroscopy to measure the absorbance at 303 nm of the HNO_3 in the organic phase as a function of HNO_3 in the contacting aqueous phase, see Figure 5.

This project has received funding from the EURATOM research and training programme 2014-2018 under grant agreement No 755171. The content of this deliverable reflects only the author's view. The European Commission is not responsible for any use that may be made of the information it contains.

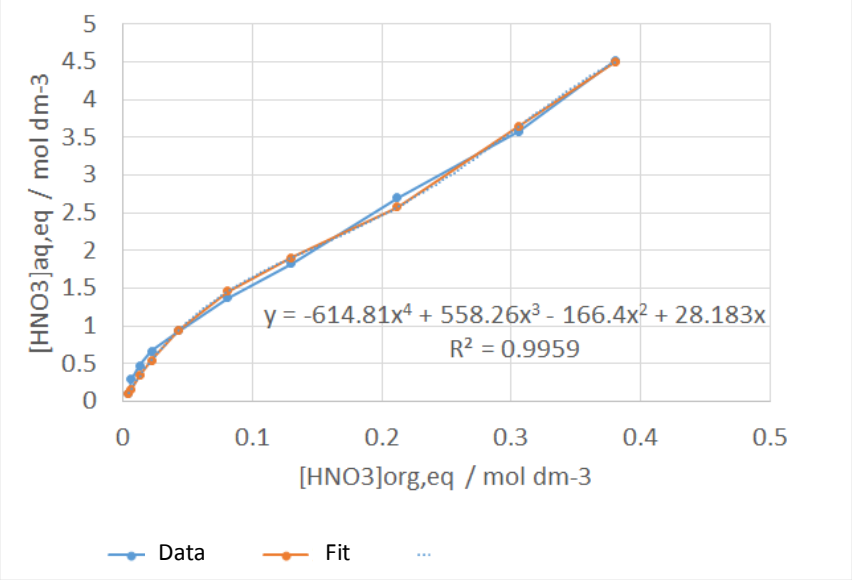

Figure 4. Blue data series: Equilibrium concentration of HNO_3 extracted into 0.2 mol dm^{-3} solution of TODGA in 5% octanol in dodecane versus the concentration of nitric acid in the aqueous phase from which the HNO_3 has been extracted (data from Geist et al, KIT). Brown data series: 4th order polynomial fit to this data, polynomial as given on figure.

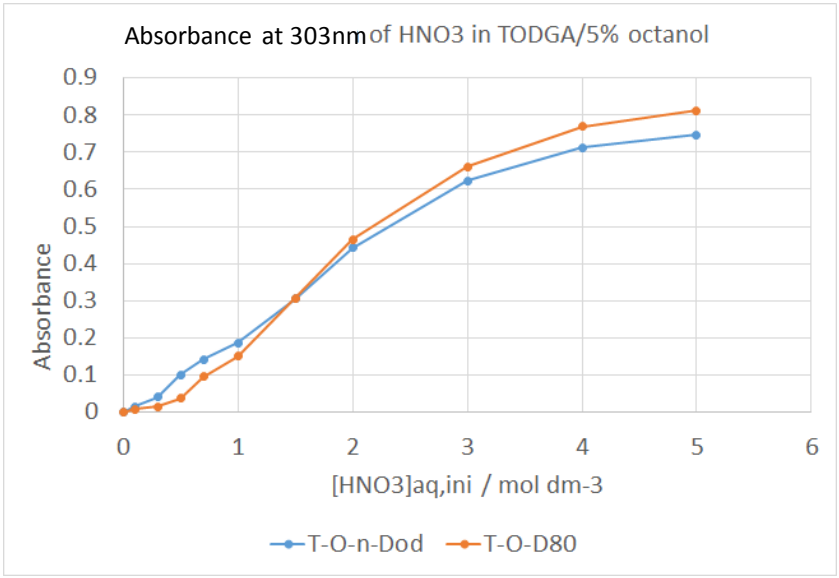

Figure 5. Absorbance at 303 nm of HNO_3 in (a) 5% octanol/dodecane (blue series) and (b) 5% octanol/exxsol D80 as a function of HNO_3 in the contacting aqueous phase.

Figures 4 and 5 can be used together to construct a calibration curve that relates the 303 nm absorbance of HNO_3 in the TODGA phase to its concentration therein, see Figure 6. This can then be used in turn to convert the HNO_3 absorbance-time data of Figure 3 to a plot of the organic phase concentration of HNO_3 as a function of time for that RDC dynamic extraction

This project has received funding from the EURATOM research and training programme 2014-2018 under grant agreement No 755171. The content of this deliverable reflects only the author's view. The European Commission is not responsible for any use that may be made of the information it contains.

experiment, see Figure 7. Figure 7 also shows the concentration of Ce(III) in the organic phase, calculated from the organic phase Ce(III) absorbance vs time data of Figure 3 using extinction coefficient data previously reported in SACSESS and referenced above. Both plots can then be used to calculate rate parameters for inter-phase transfer of Ce(III) and HNO_3 from the aqueous to organic phase. These are found to be 5 and 0.5 µm/s respectively, **indicating that the transfer of Ce(III) is more facile than that of HNO_3.**

Finally, for each data point in the $[HNO_3]_{org}$ vs t data of Figure 7, Figure 4 may be used to convert the those data points into the equivalent aqueous phase HNO_3 concentrations that would produce that concentration of HNO_3 in the TODGA phase if each data point was considered to be generated by an equilibrium extraction experiment – rather than by dynamic studies using the RDC. The so-converted data of Figure 7 is shown in Figure 8.

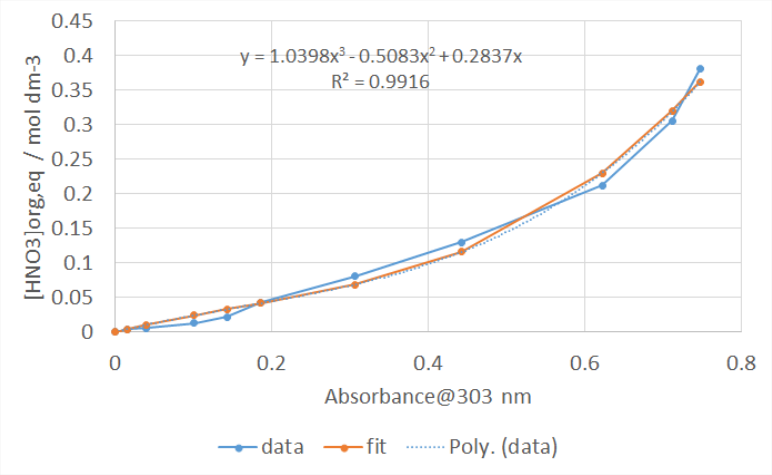

Figure 6. Concentration of HNO_3 in 5% octanol/dodecane as a function of absorbance at 303 nm of HNO_3 in that solvent.

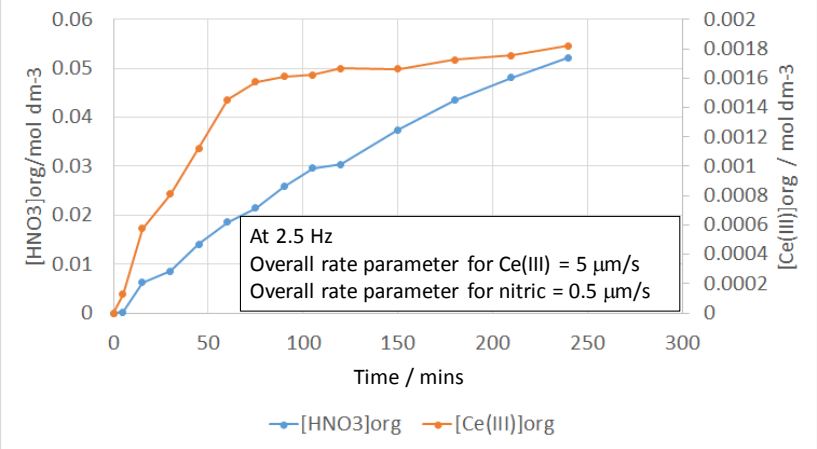

Figure 7. Dynamic extraction data of Figure 3 recast as (i) organic Ce(III) vs t data (blue series) and (ii) concentration of HNO_3 in the organic phase as a function of time (red series, see text for explanation).

This project has received funding from the EURATOM research and training programme 2014-2018 under grant agreement No 755171. The content of this deliverable reflects only the author's view. The European Commission is not responsible for any use that may be made of the information it contains.

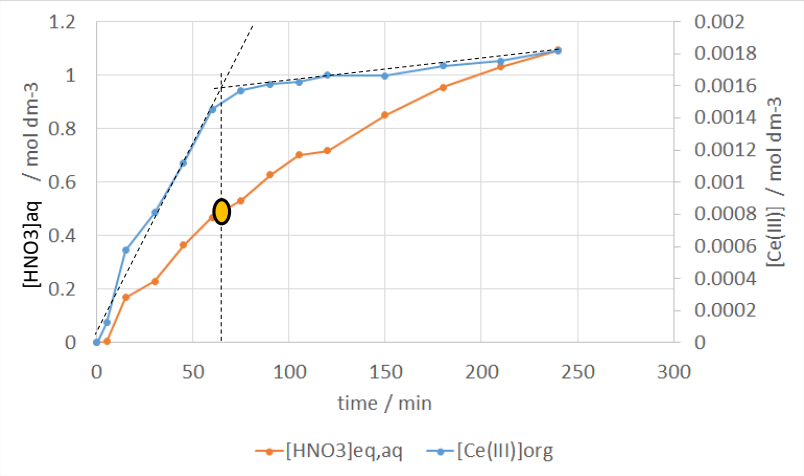

Figure 8. Dynamic extraction data of Figure 3 recast as (i) organic Ce(III) vs t data (blue series) and (ii) effective equilibrium concentration of HNO_3 in the aqueous phase as a function of time (red series, see text for explanation).

Marked on Figure 8 is the inflexion point in the Ce(III) vs t data at which Ce(III) extraction is dramatically slowed as a result of putative reverse micelle formation. Under the conditions of this particular experiment, it can be seen that this inflexion point occurs at t ≈ 65 minutes – at which point the effective equilibrium concentration of HNO_3 in the aqueous phase would be ~0.5 mol dm^{-3}. This is in reasonable agreement with the above cited work of Nave, Ganguly, Jensen, Gray and their respective co-authors who report that reverse micelle formation occurs when TODGA solutions are contacted and equilibrated with aqueous solutions of nitric acid wherein the HNO_3 concentration is ~0.7 mol dm^{-3} or greater – so supporting the conclusion that the observed inhibition of Ce(III) extraction at long contact times in the RDC experiments is indeed due to HNO_3-triggered TODGA aggregate formation in the organic phase.

A key question arising from the insights of Figures 3-8 is whether it is the acidity (i.e. proton concentration) or nitrate (NO_3^-) concentration that is responsible for the reverse micellation phenomenon. An RDC extraction experiment conducted on the Ce(III)-TODGA system using 0.5 mol.dm^{-3} HNO_3, but with total nitrate concentration of 1.0 mol.dm^{-3}, Figure 9, has provided useful insights in this regard.

This project has received funding from the EURATOM research and training programme 2014-2018 under grant agreement No 755171. The content of this deliverable reflects only the author's view. The European Commission is not responsible for any use that may be made of the information it contains.

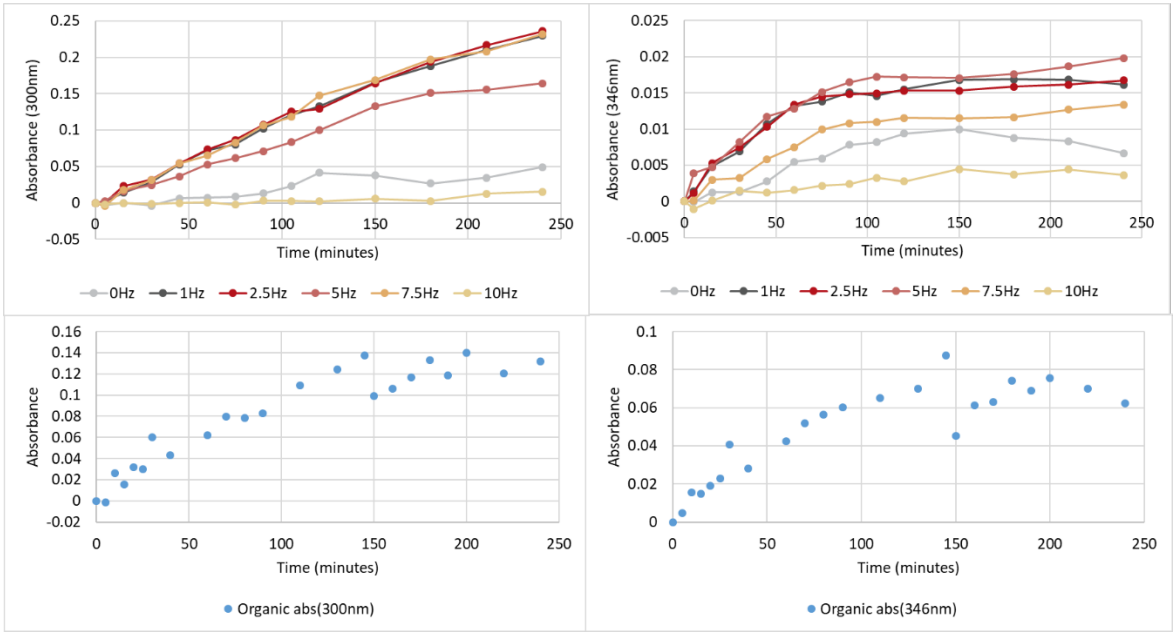

Figure 9: RDC extractions of nitrate (top left) and Ce(III) (top right) in 1 mol.dm^{-3} HNO_3 compared with 0.5 mol.dm^{-3} HNO_3 and 0.5mol.dm^{-3} $NaNO_3$ at 1Hz (bottom).

As might be expected, the data of Figure 9 shows that nitrate extraction occurs at a lower rate at the lower acidity. However, Figure 9 also shows that, at this lower acidity, Ce(III) extraction occurs both to a greater extent overall and to longer extraction times before any plateauing in extraction rate of the type observed in Figures 2 and 3 is observed.

This suggests that reverse micellation is caused to a greater extent by the acidity of the aqueous phase and not the nitrate concentration – and that this micellation can be inhibited by reducing the net proton concentration at which the extraction is conducted.

As well, the higher proton concentrations must assist the extraction of nitrate into the organic phase; thus, at lower acidities, we observe a greater overall extraction of Ce(III) due to a decrease in competition from the combination of nitrate, nitric and proton species. Since nitrate (NO_3^-), undissociated nitric acid (HNO_3) and protons (H^+) all have the potential to form part of the TODGA/metal ion complex, the experiment performed here leads to the conclusion that the proton-containing species (HNO_3 and H^+) pose more of a competition with Ce(III), in terms of being the complexation target, than lone NO_3^- ions.

4. CE(III) EXTRACTION BY TODGA – SEMI-ANALYTICAL MODELLING OF EXTRACTION RATE DATA AT SHORT EXTRACTION TIMES.

Returning to the initial extraction of Ce(III) into the organic phase, occuring at times below 60 minutes (Figure 2), it is in this region that the putative reverse micellation in the organic

This project has received funding from the EURATOM research and training programme 2014-2018 under grant agreement No 755171. The content of this deliverable reflects only the author's view. The European Commission is not responsible for any use that may be made of the information it contains.

phase is theoretically kept at bay by the low transfer of nitric acid, and associated species, into the organic phase. Thus, the mass transfer and chemical kinetic behaviour may be better interrogated.

The existing dataset of Ce(III) extractions in the RDC (Figure 2), performed at different rotation speeds, shows a flux (j) dependence on rotation speed (Figure 10) that is counter-intuitive to two-film theory. Specifically, as membrane rotation speed is increased (so increasing the rate of convective mass transfer of the Ce(III) in the aqueous phase to the membrane surface), the extraction flux goes *down*. For this reason an alternative model to explain the extraction behaviour has been derived.

Given the inverse dependence of extraction rate on membrane rotation speed, for the purposes of creating a model for the mass transfer and chemical kinetics of the RDC initial extraction region (Figure 2), we have worked in terms of extraction flux (j) of the TODGA/metal ion complex over the RDC membrane as a function of inverse square root of rotation speed (Figure 10).

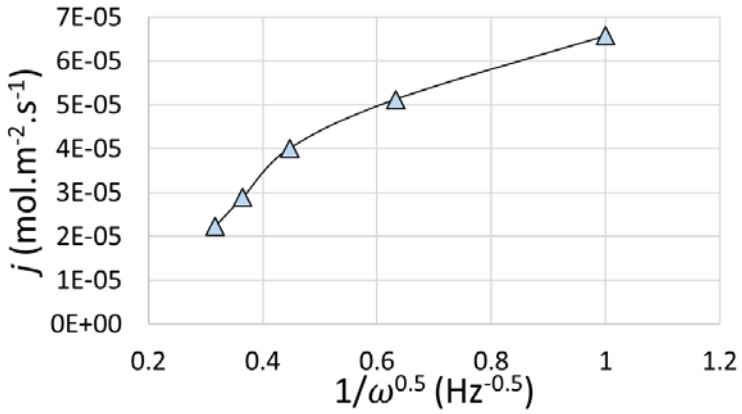

Figure 10: Extraction flux (j) of Ce(III) into the organic phase as a function of inverse square root of rotation speed ($1/\omega^{0.5}$) calculated using the short extraction time data of Figure 2

As alluded to above, a simple two-film theory model of the extraction rate dependence on membrane rotation speed predicts the opposite trend to the one exhibited by the RDC. The alternative model to two-film theory presented here, with which we are able to describe RDC extraction, is analytical in nature but has incorporated numerical modelling tools for the purposes of parameter estimation.

The mass transfer with chemical reaction (MTWCR) scheme underlying the analytical model assumes that the TODGA ligand (L) from the organic phase migrates into a stagnant diffusion layer in the aqueous phase to complex with the metal ions (M) in solution, forming a ligand/metal complex (C). Equations 1 and 2 show the fundamental diffusion-reaction

This project has received funding from the EURATOM research and training programme 2014-2018 under grant agreement No 755171. The content of this deliverable reflects only the author's view. The European Commission is not responsible for any use that may be made of the information it contains.

equations for L and C as a function of M and distance x from the membrane interface into the aqueous stagnant diffusion layer. The thickness of this diffusion layer (X_D) is a function of rotation speed (ω) prescribed by the Levich Equation ($X_D = 0.643\omega^{-\frac{1}{2}}\upsilon^{\frac{1}{6}}D_L^{\frac{1}{3}}$, where υ is viscosity and ω is in units of Hz). The model assumes a 1:1 stoichiometry between L and M with k_f ($mol^{-1}.m^3.s^{-1}$) and k_b (s^{-1}) representing the forwards and backwards reaction rate of the complexation reaction, respectively. Other key parameters include D_L and D_C ($m^2.s^{-1}$); the diffusivities of L and C, respectively. We assume that M is in a large excess in the aqueous phase, hence no equation for M is required and we can write that $k_f' = k_f M$ i.e. a pseudo-first order rate parameter for complex formation may be used.

$$D_L \frac{d^2L}{dx^2} - k_f'L + k_bC = 0 \quad (1)$$

$$D_C \frac{d^2C}{dx^2} + k_f'L - k_bC = 0 \quad (2)$$

Equations 3 and 4 describe the model solutions to the ligand and complex concentration profile as a function of χ (where $\chi = x/X_D$). Equations 5 to 8 describe the constant terms *A*, *B*, *G* and *H* in the solution profiles and include all boundary conditions; L_i, C_i, L_D and C_D. L_i and C_i are the concentrations of ligand and complex, respectively, at $x = 0$ and L_D and C_D are likewise but for $x = X_D$.

$$L = Ae^{\xi\chi} + Be^{-\xi\chi} \quad (3)$$

$$C = Ge^{\kappa\chi} + He^{-\kappa\chi} - \frac{\xi^2 L}{\xi^2 - \kappa^2} \quad (4)$$

$$A = L_i - B \quad (5)$$

$$B = \frac{L_D - L_i e^{\xi}}{e^{-\xi} - e^{\xi}} \quad (6)$$

$$G = C_i - H + \frac{\xi^2 L_i}{\xi^2 - \kappa^2} \quad (7)$$

$$H = \frac{C_D - C_i e^{\kappa} - \frac{\xi^2}{\xi^2 - \kappa^2}(L_i e^{\kappa} - L_D)}{e^{-\kappa} - e^{\kappa}} \quad (8)$$

The dimensionless parameters ξ and κ in Equations 3 to 8 are defined as follows: $\kappa = X_D/X_k$, $\xi = X_D/X_f$, $X_f = \sqrt{D_L/k_f M}$ and $X_k = \sqrt{D_C/k_b}$. X_f and X_k are the forwards and backwards reaction lengths, respectively.

This project has received funding from the EURATOM research and training programme 2014-2018 under grant agreement No 755171. The content of this deliverable reflects only the author's view. The European Commission is not responsible for any use that may be made of the information it contains.

The equation to convert the complex concentration profile (C), Equation 4, to the flux of Ce(III) extracted into the organic phase (j) is simply the derivative with respect to x and χ at $x = 0$, shown by Equation 9.

$$j = D_C \frac{dC}{dx}\Big|_{x=0} = \frac{D_C}{X_D}\frac{dC}{d\chi}\Big|_{\chi=0} \quad (9)$$

As with any solutions to differential equations, the model requires the specification of the boundary conditions. L_D and C_D may be set to zero, owing to the large volume of the convective mixing region beyond the diffusion layer and L_i may be set to the literature value (Sasaki, 2001) for TODGA solubility (0.042 mmol.dm^{-3}). C_i, in the first instance, was set to zero due to the assumption that the transfer of complex into the organic phase occurred sufficiently fast so as to reduce the interface concentration to approximately zero. (In reality, this turns out to be too great a simplification and the process of assigning a value to C_i is the subject of Section 5).

To quantify how accurately the model fits the experimental data, Equations 3 to 9 have been coded in the gPROMS parameter estimation software. The literature value of 2.00x10^{-9} m^2.s^{-1} for D_C (Simonin, 2015) was used as a seed value for the gPROMS parameter estimator, as was the literature value (Sasaki, 2001) for L_i, in order that the parameters k_f and k_b could be estimated.

Unfortunately, the parameter estimator failed to converge on values for k_f and k_b without the necessity of raising L_i from the literature value of 0.042 mmol.dm^{-3} to a value 10 to 100 times greater than this. Similarly, keeping L_i close to the literature value of 0.042 mmol.dm^{-3} could only be achieved by raising the complex diffusivity (D_C), which is 2.00x10^{-9} m^2.s^{-1} in the literature, to a value in the order of 10^{-8} to 10^{-7}; which would not be physically achievable in our system.

At the time of these parameter estimation runs, it was speculated that the presence of 5% octanol, a phase modifier, in the organic phase could be increasing the solubility of TODGA in HNO_3. Due to our arrival at this hypothesis, and the fact that octanol influence on a TODGA system has been largely understudied, a determination of TODGA solubility in HNO_3 was the necessary next step.

This project has received funding from the EURATOM research and training programme 2014-2018 under grant agreement No 755171. The content of this deliverable reflects only the author's view. The European Commission is not responsible for any use that may be made of the information it contains.

5. MALDI TOF MASS SPECTROSCOPY STUDY OF TODGA SOLUBILITY IN HNO_3

MALDI TOF mass spectrometry is a method which can be used to quantify very small concentrations of solutes in solution and, since TODGA is widely viewed as being sparingly soluble in water and nitric acid (~0.042mmol.dm^{-3}), has been used to estimate TODGA concentrations in HNO_3 (Khesina, 2017). The MALDI TOF method of mass spectrometry carries the same principles as other mass spectrometry, i.e. the ionisation of the molecules in a sample and deduction of the mass to charge ratio (m/z) based on measurements of time of flight in a magnetic field. The only difference between other methods and MALDI TOF is that MALDI TOF uses manually directed laser shots as the means of ionisation and subsequent desorption from a dried liquid matrix on a steel sample plate.

Since we are interested in interrogating the effect of the presence of octanol on TODGA solubility in the aqueous phase, 1 mol.dm^{-3} HNO_3 solutions were contacted with a range of octanol concentrations (5-50%) in pure TODGA in an Eppendorf Thermomixer at 25°C to provide acid samples saturated with TODGA at the solubility limit. The TODGA in the acid samples was subsequently back extracted into HPLC grade hexane before being diluted in a solvent of water (10 vol% trifluoroacetic acid (TFA)) and acetonitrile (AcN). TFA provides a source of protons to protonate the laser-ionised TODGA and to encourage a more uniform crystalisation when the sample droplets are drying on the metal plate to be loaded into the MALDI TOF vacuum chamber. This is important as it ensures there are no solute-rich regions within a single sample spot, thus being unreflective of the concentration of the solute in the original sample. To further ensure uniform crystalisation, a droplet of liquid matrix is added to each sample spot on the MALDI plate. The matrix used was 2,5-dihydroxybenzoic acid (DHB) dissolved in the same solvent mixture as the sample.

After the sample plate has been loaded into the MALDI TOF and the vacuum has been established, a laser is manually directed at the sample spots using a camera. Though the aforementioned steps were taken to avoid solute 'hot spots', they were still encountered, thus the average m/z peak at ~581 Da (the m/z of TODGA), was calculated from a range of laser shots directed at a minimum of 6 locations on each sample spot. The Shimadzu Axima iDplus Performance MALDI-TOF mass spectrometer at ULANC was utilised for these experiments.

The purpose of these experiments was to see whether the presence of octanol in the organic phase increased TODGA solubility in the aqueous phase but the results (Figure 11) revealed that this is not the case. Whilst the error bars are large for some of the data (due to the low concentrations of TODGA being interrogated) two key observations can be made.

1. The concentration of TODGA in the aqueous phase is broadly independent of the concentration of octanol in the organic phase; and

This project has received funding from the EURATOM research and training programme 2014-2018 under grant agreement No 755171. The content of this deliverable reflects only the author's view. The European Commission is not responsible for any use that may be made of the information it contains.

2. The aqueous concentrations of TODGA observed experimentally here are broadly in line with that reported in the literature ~0.042 mmol dm^{-3}.

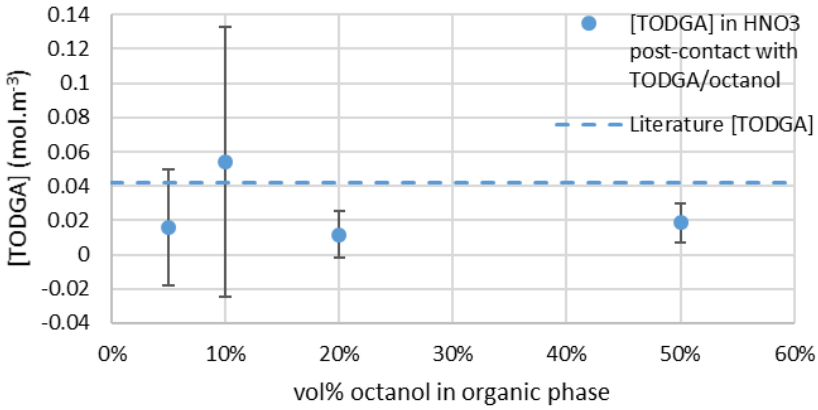

Figure 11: Concentration of TODGA in HNO_3 at different octanol concentrations estimated by MALDI TOF mass spectrometry

In light of the aqueous TODGA solubility values presented in Figure 11, the model of section 3 was revisited – this time with only those parameters with values reported in the literature being fixed. This is discussed in the next section.

6. CE(III) EXTRACTION BY TODGA – NUMERICAL MODELLING OF EXTRACTION RATE DATA AT SHORT EXTRACTION TIMES.

As stated above, the MALDI-TOF MS determined value for the aqueous solubility of TODGA led us to revisit the model of section 3 – this time only fixing those boundary conditions or implicit constants that have values reported in the literature. Only the aqueous solubility of TODGA, corresponding to the boundary condition L_i, and the diffusion coefficient of the complex, corresponding to the implicit constant D_C, are so defined. This means that all other boundary conditions and implicit constants, D_L, C_i, k_f and k_b, must be left to float during fitting of the model to the experimental Ce(III) extraction flux-membrane rotation speed data of Figure 10. The fitting of such a large number of parameters requires use of a numerical rather than analytical approach.

Thus, using the equations (3)-(9) of section 3, the gPROMS parameter estimator was used to converge on values of D_L, C_i, k_f and k_b,, and test whether a good experimental fit could be achieved whilst maintaining the literature values for the complex diffusivity and TODGA solubility. The results of this parameter estimation process are given in Table 1 with the associated modelled fit to the experimental data being shown in Figure 12.

This project has received funding from the EURATOM research and training programme 2014-2018 under grant agreement No 755171. The content of this deliverable reflects only the author's view. The European Commission is not responsible for any use that may be made of the information it contains.

Table 1: Parameter estimation results for analytical model with floating C_i boundary condition.

k_f (mol^{-1}.m^{3}s^{-1})	363 ± 42
k_b (s^{-1})	1.00x10^{-4}
L_i (mmol.dm^{-3})	0.042 [2]
C_i (mmol.dm^{-3})	1.037 ± 0.098
D_L (m^2.s^{-1})	3.71x10^{-9}
D_C (m^2.s^{-1})	2.00x10^{-9} [3]

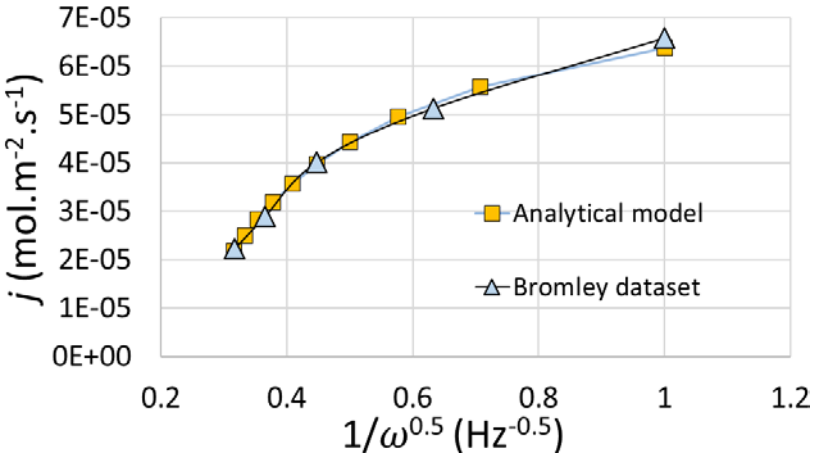

Figure 12: Modelled extraction flux (j), with associated parameter results in Table 1, as a function of inverse square root of rotation speed ($1/\omega^{0.5}$).

The following can be seen from Table 1 and Figure 12:

- The maximum observed extraction flux of 6.6 x 10^{-5} mol m^{-2} s^{-1} at a membrane rotation speed of 1 Hz for 10 mmol.dm^{-3} Ce(III) gives an extraction rate of 6.6 µm s^{-1}. This is rather fast and is comparable to interfacial rate parameters for TODGA/Am^{3+} & Eu^{3+} extractions of 31 µm s^{-1} (Simonin, Boxall, Lélias, 2015)
- C_i converges on a value of 1.037 mmol.dm^{-3}, approximately 10% of the total metal ion concentration in the aqueous phase. Crucially, this is an achievable boundary condition physically in the sense that there is a large supply of metal ions able to feed the complexation reaction occurring in the aqueous diffusion layer.

This project has received funding from the EURATOM research and training programme 2014-2018 under grant agreement No 755171. The content of this deliverable reflects only the author's view. The European Commission is not responsible for any use that may be made of the information it contains.

- D_L converges on a value approximately twice that of the literature value of the complex diffusivity D_C, which is also a sensible result as free TODGA is a smaller molecule than the complex, hence is likely to be more diffusible.
- k_f converges on a value of 363 ± 42 $mol^{-1}.m^3.s^{-1}$ for Ce^{3+}/TODGA complex formation in the aqueous phase. This is a factor of 10 more than the values of 10-30 m^3 mol^{-1} s^{-1} reported for Ln^{3+} with DTPA (Nash et al) and 12-55 m^3 mol^{-1} s^{-1} reported for Eu^{3+} with DTPA (Mezyk & Martin). This value of k_f corresponds to a complex formation length, X_f, of 1 µm – meaning that complexation occurs close to the aqueous-organic interface and within distances less than the RDC diffusion layer thickness, X_D, which, for this system ranges from 81 µm at a rotation rate of 1 Hz to 11 µm at a rotation rate of 49 Hz.
- From sensitivity studies and model troubleshooting, k_b was found to have a negligible effect on the flux values output from the model, hence this was simply fixed at a small non-zero value of 1.00×10^{-4} s^{-1} for the purposes of this parameter estimation run. This corresponds to a decomplexation length, X_k, of more than 4 mm i.e. once the complex has been formed, it is very stable and can diffuse longer distances than the thickest diffusion layer employed in these experiments.

Other kinetic studies using alternative experimental equipment designs such as the Rotating Membrane Cell (RMC) use Nd(III) as the trivalent actinide analogue, instead of Ce(III). In order for the reaction constants obtained using the RDC to be compared with the values produced by these other methods, an RDC study of the Nd(III)-TODGA extraction system has begun. These are at an early stage and will not be reported in here. However, supporting rotary mixer studies of the distribution ratios of the Nd(III)-TODGA system are well advanced, providing insights into the stoichiometry of the extracted complex. These are presented in the next section.

7. EXTRACTION OF ND(III) USING TODGA: ROTARY MIXER STUDIES

As discussed above, other kinetic studies use Nd(III) instead of Ce(III) as the extracted metal ion. We have identified some of the main reasons for switching to Nd(III), including the fact that the UV-vis absorbance peaks for the metal ion in the organic phase emerge at a wavelength far away from the nitrate peak, whereas the Ce(III) absorbance peak appears very near the tail of the nitrate peak. As well as this, as mentioned in Section 5, the RDC kinetic data may be compared with other studies which use Nd(III).

This project has received funding from the EURATOM research and training programme 2014-2018 under grant agreement No 755171. The content of this deliverable reflects only the author's view. The European Commission is not responsible for any use that may be made of the information it contains.

Initial mixer settler experimental studies of the TODGA extraction of Nd(III) have been conducted with the principal aim of determining the stoichiometry p of the following complexation reaction:

$$p\mathrm{TODGA}_{org} + q\mathrm{NO_3^-}_{aq} + \mathrm{Nd}^{3+}_{aq} \leftrightharpoons \mathrm{TODGA}_p(\mathrm{NO_3^-})_q\mathrm{Nd}^{3+}_{org} \quad (10)$$

The equilibrium relation which can be drawn from Equation 10 is shown below (Equation 11).

$$K_{D_{\mathrm{Nd}^{3+},eq}} = \frac{\left[\mathrm{Nd}^{3+}\mathrm{TODGA}_p(\mathrm{NO_3^-})_q\right]_{org}}{[\mathrm{Nd}^{3+}]_{aq}[\mathrm{NO_3^-}]^q_{aq}[\mathrm{TODGA}]^p_{org}} \quad (11)$$

For the experiment, 1.0mL of aqueous and 0.9mL of organic solution were pipetted into 2.0mL Eppendorf vials. The vials were then loaded into an Eppendorf Thermomixer, mixed for 20 minutes at 25°C and centrifuged for 5 minutes. The UV-vis spectrum of the produced organic phase was taken and the absorbance peak at 584nm was used to determine $\left[\mathrm{Nd}^{3+}\mathrm{TODGA}_p(\mathrm{NO_3^-})_q\right]_{org}$ (organic Nd(III) concentration). As well as this, the absorbance spectrum of the aqueous phase was taken and $[\mathrm{Nd}^{3+}]_{aq}$ was calculated from the peak at 740nm. Since $D_{\mathrm{Nd}^{3+}} = \left[\mathrm{Nd}^{3+}\mathrm{TODGA}_p(\mathrm{NO_3^-})_q\right]_{org} / [\mathrm{Nd}^{3+}]_{aq}$ Equation 12 can be formed.

$$D_{\mathrm{Nd}^{3+}} = K_{D_{\mathrm{Nd}^{3+},eq}}[\mathrm{NO_3^-}]^q_{aq}\,[\mathrm{TODGA}]^p_{org} \quad (12)$$

A range of mixer settler experiments, performed at different organic TODGA concentrations, with the same aqueous Nd(III) concentration, allows the determination of stoichiometric constant p using a log/log plots of Equation 12 (which is shown by Equations 13).

$$\log(D_{\mathrm{Nd}^{3+}}) = \log\left(K_{D_{\mathrm{Nd}^{3+},eq}}\right) + p\log[\mathrm{TODGA}]_{org} + q\log[\mathrm{NO_3^-}]_{aq} \quad (13)$$

A value of $p \approx 2.30$ (Figure 13) is lower than the findings of the literature (Nave, 2004; Zhu, 2004; Whittaker, 2018), which predict that there are a mixture of predominantly 3:1 and 4:1 complexes of TODGA/Nd(III) produced in the extraction process. However, the study cited primarily, that looks at coordination number (Zhu, 2004), uses HNO_3 concentrations of 3.0mol.dm^{-3} . The value found in our experiments suggests a mixture of predominantly 2:1 and 3:1 which could be lower than the literature due to the lower acidity used.

A pertinent question remains as to whether the rate determining step in the overall complex formation is the initial 1:1 complexation step. If this is the case, the modelling work presented here is valid and can be applied to this system. If the rate determining step is a different or a combination of all the complexation steps, the model will need to be modified

This project has received funding from the EURATOM research and training programme 2014-2018 under grant agreement No 755171. The content of this deliverable reflects only the author's view. The European Commission is not responsible for any use that may be made of the information it contains.

further to incorporate higher stoichiometries. Also, the model as yet does not factor in the transport and kinetics of NO_3^-, which is justifiable since it is in a huge excess, but, since it can be shown to be a part of the complexation process, the model must be deployed with the acknowledgment of such limits.

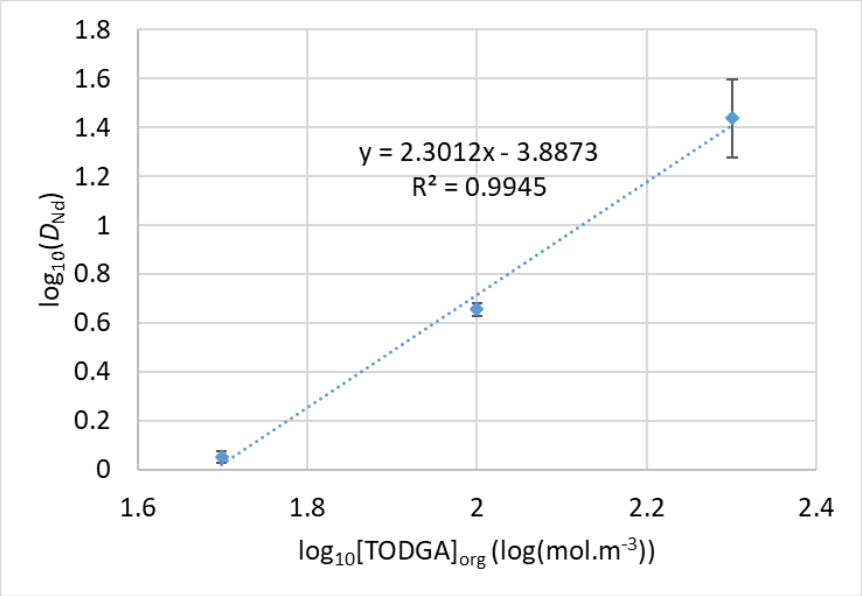

Figure 13: log(D_{Nd}) vs log$[TODGA]_{org}$ (mixer/settler of 10mmol.dm^{-3} Nd^{3+} in 1.0 mol.dm^{-3} HNO_3 with TODGA (50, 100, 200 mmol.dm^{-3}) in n-dodecane (5% octanol)).

To conclude, the rotary mixer studies shed light on what the formed complexes of TODGA/Nd(III)/NO_3^- look like.

- Based on the data, we predict 2 to 3 TODGA molecules are complexed per 1 ion of Nd(III), which is not consistent with the original coordination study (Zhu, 2004) which suggests 3 or 4 TODGA molecules per ion. However, the acidity used in our experiments (1 mol.dm^{-3}) is lower than used in the literature (3mol.dm^{-3}) (Zhu, 2004), thus the lower coordination number reported here could be a manifestation of the lower extraction capability of TODGA at lower nitrate conditions, which is reported in the literature (Whittaker, 2018).
- These experiments reveal that the structure of the TODGA/Nd(III)/NO_3- complex at equilibrium is not simply 1:1 with respect to TODGA and Nd(III). The model used to predict the kinetics (described in Sections 3 and 5) may still be applied, despite its underlying assumption of a 1:1 complex, as long as the rate determining step can be shown to be the 1:1 initial complexation reaction. These kinetic studies will be better investigated using the RDC. These studies are ongoing presently.

This project has received funding from the EURATOM research and training programme 2014-2018 under grant agreement No 755171. The content of this deliverable reflects only the author's view. The European Commission is not responsible for any use that may be made of the information it contains.

8. CONCLUSIONS AND FURTHER WORK

To summarise the content of this report, there are several key areas for which questions have been answered - but which also give rise to new areas of inquiry.

For **Rotation speed studies at short extraction times** indicate the following**:**

- The ligand/metal ion reaction is not occurring at the interface – but very close to it in a stagnant diffusion later in the aqueous phase.
- The extent of the diffusion of ligand into the aqueous phase has been found to be greater than the reaction length of complexation, and this in turn is greater than the diffusion range of complex. From this we can say that the system can be described by MTWCR.
- The formed complex is long lived.
- The initial extraction rate is **proportional to [Ce^{3+}], [HNO_3]** (determined in SACSESS)
- The Extraction can be inhibited by high shear i.e. the effect of the stagnant diffusion layer becoming so small that loss of complex to bulk is encountered.
- The maximum observed extraction flux of 6.6 x 10^{-5} mol m^{-2} s^{-1} at a membrane rotation speed of 1 Hz for 10 mmol.dm^{-3} Ce(III) gives an extraction rate of 6.6 μm s^{-1}. This is rather fast and is comparable to interfacial rate parameters for TODGA/Am^{3+} & Eu^{3+} extractions of 31 μm s^{-1} (Simonin, Boxall, Lélias, 2015)

For **Rotation speed studies at long extraction times,** the following has been found**:**

- Increasing [HNO_3] increases initial extraction rate but leads to reverse micellation at critical organic acidity of 20 mmol.dm^{-3}.
- HNO_3 aids the thermodynamic extent of extraction but hinders kinetics (rate of extraction).
- Due to the above effects of HNO_3 there will be implications for solvent re-use, i.e. processing steps to back extract nitrate from the organic phase may be necessary.

The **Low acidity (0.5M HNO_3 + 0.5M $NaNO_3$) study** indicates**:**

- **Less nitrate is extracted** whilst **Ce(III) is extracted faster, for longer** and **to a greater extent**, implying that the nitrate component of the formed complex requires a free proton or for a dissociated acid molecule to be present (HNO_3).
- **Acidity is key** to micelle formation phenomenon, not just NO_3^- concentration.

This project has received funding from the EURATOM research and training programme 2014-2018 under grant agreement No 755171. The content of this deliverable reflects only the author's view. The European Commission is not responsible for any use that may be made of the information it contains.

The **rotary mixer** work on the **variation of [TODGA] to obtain order with respect to TODGA**, has revealed:

- The stoichiometry with respect to **TODGA is 2 to 3 molecules per Nd(III)** ion**.**
- This differed from the literature (Zhu, 2004), however the acidity used in the experiments at ULANC was 1 $mol.m^{-3}$ rather than 3 $mol.m^{-3}$, thus the stoichiometry results here may be indicative of the reduced extraction behaviour expected at lower nitric acid concentrations.

The **kinetic modelling work** has revealed:

- The homogeneous rate of complex formation, k_f = **363 ± 42 $m^3.mol^{-1}.s^{-1}$**
- The rate of decomplexation, k_b = **~0.0001s^{-1}**
- Literature TODGA aqueous solubility of **0.042 mmol dm^{-3}** and complex diffusivity of **2.0x10^{-9} $m^2.s^{-1}$** are accurate parameters for the model – and **supported by MALDI TOF mass spectroscopy experiments**
- Interface complex concentration C_i now estimated to be **1.037 ± 0.098 $mmol.dm^{-3}$**

The **future work** in the remainder of this PhD studentship at ULANC and, potentially beyond, includes:

- Pre-contacted TODGA with nitric acid to establish kinetics of extraction into recycled solvent.
- RDC runs of Nd(III) to compare with other workers in GENIORS
- The effects of different components of the organic phase need to be investigated such as:
    - The phase modifier octanol,
    - The branched diluent TPH,
    - The branched ligand - T2EHDGA
    - And the newest synthesised TODGA variant: mTDDGA.
- Mixed TODGA/DMDOHEMA systems are also future experiments to be performed.
- Finally, rather than focusing solely on extraction conditions, the stripping kinetics of SO_3-Ph-BTBP / SO_3-Ph-BTP / SO_3-Ph-BTPhen / AHA systems would be a valuable insight.

This project has received funding from the EURATOM research and training programme 2014-2018 under grant agreement No 755171. The content of this deliverable reflects only the author's view. The European Commission is not responsible for any use that may be made of the information it contains.

REFERENCES

Bromley, M. & Boxall, C. (2015), 'A study of cerium extraction by TBP and TODGA using a rotating diffusion cell', *Nukleonika* **60**(4), 859–864.

Nave, S., Modolo, G., Madic, C., & Testard, F. (2004), 'Aggregation Properties of N,N,N',N'-Tetraoctyl-3-oxapentanediamide (TODGA) in n-Dodecane', *Solvent Extraction and Ion Exchange* **22**(4), 527-551.

Jensen, M., Yaita, T., & Chiarizia, R. (2007) 'Reverse-micelle formation in the partitioning of trivalent F-element cations by biphasic systems containing a tetraalkyldiglycolamide', *Langmuir : The ACS Journal of Surfaces and Colloids* **23**(9), 4765-4774.

Ganguly, R., Sharma, J., & Choudhury, N. (2011) 'TODGA based w/o microemulsion in dodecane: An insight into the micellar aggregation characteristics by dynamic light scattering and viscometry', *Journal of Colloid And Interface Science*, **355**(2), 458-463.

Sasaki, Y., Sugo, Y., Suzuki, S. & Tachimori, S. (2001), *Solvent Extraction and Ion Exchange* **19**(1), 91–103.

Nash, K., Brigham, D., Shehee, T., & Martin, A. (2012). The kinetics of lanthanide complexation by EDTA and DTPA in lactate media. *Dalton Transactions,* **41**(48), 14547-14556.

Larsson, K., & Mezyk, S. (2018). Dissociation rate kinetics of europium-DTPA complexes. *Journal of Radioanalytical and Nuclear Chemistry,* **318**(1), 649-652.

Simonin, J.-P. , Boxall, C. & Lelias, A. (2015), 'SACSESS deliverable D12.5 - kinetics of extraction and stripping', *European Commission*.

Khesina, Z., Iartsev, B., Pytskii, S., Goncharova, D., Paramonov, I., Milutin, A., Buryak, N. (2017), 'Study of the possibility of quantitative analysis of N , N , N ', N '-tetra- n -octyldiglycolamide by MALDI mass spectrometry', *Russian Chemical Bulletin* **66**(6), 995-998.

Zhu, Z., Sasaki, Y., Suzuki, H., Suzuki, S., & Kimura, T. (2004) 'Cumulative study on solvent extraction of elements by N, N, N', N'-tetraoctyl-3-oxapentanediamide (TODGA) from nitric acid into n-dodecane', *Analytica Chimica Acta*, **527**(2), 163-168.

Whittaker, D., Geist, Modolo, Taylor, Sarsfield, & Wilden (2018) 'Applications of Diglycolamide Based Solvent Extraction Processes in Spent Nuclear Fuel Reprocessing, Part 1: TODGA', *Solvent Extraction and Ion Exchange*, **36**(3), 223-256.

This project has received funding from the EURATOM research and training programme 2014-2018 under grant agreement No 755171. The content of this deliverable reflects only the author's view. The European Commission is not responsible for any use that may be made of the information it contains.

STUDY OF EXTRACTION AND STRIPPING KINETICS OF EUROPIUM(III) AND AMERICIUM(III) BY THE EXTRACTANTS TODGA AND CYME$_4$-BTBP

CNRS-PHENIX

T.H. Vu and J.P. Simonin, Laboratoire PHENIX, CNRS-Sorbonne Université, Paris, France

1. INTRODUCTION

We have performed extraction kinetics experiments of Eu(III) and Am(III) ions for various compositions of the aqueous and organic phases. The latter was composed of the extractants TODGA or CyMe$_4$-BTBP, or of mixtures of these molecules, in TPH.

The experiments were carried out using the rotating membrane cell (RMC) technique (see section II). An experiment with this technique can be carried out in two different ways: (*i*) extraction in which the aqueous phase containing the radioactive solute is placed in the membrane and the external phase is organic; (*ii*) stripping where the organic solution containing the radioactive solute is in the membrane, and the external phase is aqueous.

Here, the two ways (extraction/stripping) were generally employed and it was checked that they gave similar results for the rate constants.

In previous works we have used the Durapore hydrophilic membrane from Millipore. New types of membranes have been used in this study. They give results for the diffusion coefficients (denoted by *D* throughout) that are now more consistent with those obtained using the closed capillary technique[1].

2. THE ROTATING MEMBRANE CELL (RMC) TECHNIQUE

The RMC technique is depicted in Figure 1. The cell consists of a thin membrane that is glued on the base of a cylinder made of Perspex.

The phase (aqueous or organic) containing the radioactive solute (^{152}Eu, ^{241}Am) is always placed in the membrane initially (phase A). The cell is mounted on a rotating-electrode spindle[2,3] that is rotated at a definite speed. At time t=0, it is set into rotation and then it is immersed into the outer phase B.

This project has received funding from the EURATOM research and training programme 2014-2018 under grant agreement No 755171. The content of this deliverable reflects only the author's view. The European Commission is not responsible for any use that may be made of the information it contains.

In what follows, we will assume that the reaction between the metal ion and the extractant occurs strictly at the interface between the two immiscible phases.

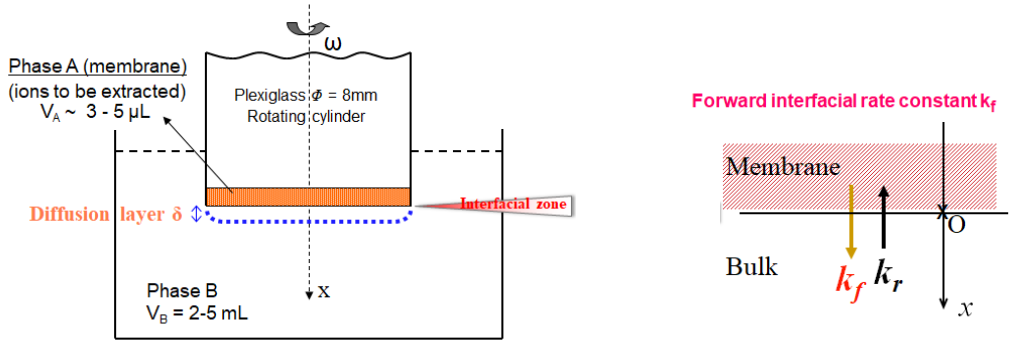

Figure 7 : Sketch of the RMC technique (left) and meaning of the interfacial rate constants (right).

In that case, the proportion of matter extracted as a function of time can be written as,

$$P(t) = 1 - \exp(-t / \tau) \quad \text{or} \quad \mathbf{-\ln[1-P(t)] = t / \tau} \tag{1}$$

where τ is the mean-passage time of the solute from the bulk of A to the bulk of B. It is given by,

$$\tau = \tau_A + \tau_f + \tau_B \tag{2}$$

in which τ_A is the mean diffusion time in phase A (the membrane), τ_f is the characteristic time for the A-to-B interfacial chemical reaction, and τ_B is the mean diffusion time in the diffusion layer in B (competition between back-extraction and removal from the interfacial region into the bulk of B),

$$\tau_f = \frac{L}{k_f} \qquad \tau_A = \frac{L^2 \theta}{3 D_A} \qquad \tau_B = \frac{\sigma L \delta_B}{K D_B} \tag{3}$$

with L is the membrane thickness, k_f the forward kinetic rate constant for the A-to-B interfacial transfer (see Fig. 1), D_A and D_B the diffusion coefficients of the solute in phases A and B, respectively, θ the tortuosity of the membrane, σ its porosity, δ_B the diffusion layer thickness in phase B, and K the distribution ratio, which besides satisfies the relation,

$$K = \frac{k_f}{k_r} \tag{4}$$

This project has received funding from the EURATOM research and training programme 2014-2018 under grant agreement No 755171. The content of this deliverable reflects only the author's view. The European Commission is not responsible for any use that may be made of the information it contains.

with k_r the reverse kinetic rate constant for B-to-A interfacial transfer. Thus, if A is aqueous and B is organic phase, then k_f and k_r are the extraction rate constant and the stripping rate constant, respectively.

In the case of infinitely fast interfacial kinetics (k_f and $k_r \rightarrow \infty$: $\tau_f \rightarrow 0$, with K unchanged), the process becomes diffusion controlled and Eq. 2 reduces to :

$$\tau_\infty = \tau_A + \tau_B \qquad (5)$$

Replacing τ by τ_∞ in Eq. (1) yields the diffusive limit, P_∞, of the process.

The determination of the contributions from transport in phases A and B requires the measurement of the diffusion coefficients of solute, D_A and D_B, in the two phases. They were generally determined using the RMC. There were also measured using the closed capillary technique in some cases for comparison. With the RMC, the phases A and B are identical (so $D_A \equiv D_B = D_{solute}$), then the process is simply a diffusion of the solute from A to B, so that $\tau_f = 0$ (no reaction) and the distribution ratio value is K=1. Since the parameters (L, σ, ν_B, ω) are determined independently, Eqs. 1-3 and 5 allow the calculation of D_{solute} from the RMC experimental value of τ, if the tortuosity is known. Thus, conversely, if D_{solute} is known, the tortuosity of the membrane can be determined.

3. EXPERIMENTAL

1. CHEMICALS, MEMBRANES AND METHODS

The extractants TODGA and $CyMe_4$-BTBP, the complexing agents SO_3-Ph-BTP and PTD, and the TPH diluent were supplied by GENIORS partners: Wim Verboom, Andreas Geist, Alessandro Casnati, and CEA, respectively; they were used without further purification. The ^{152}Eu(III) and ^{241}Am(III) radioactive sources were purchased from ORANO-LEA (France). Aqueous solutions were prepared with ultrapure water (Millipore, 18.2 MΩ·cm). All other chemicals were purchased from AnalaR (Normapur®), Sigma-Aldrich or Fluka, and were used as received.

The distribution ratios were determined by equilibrating 500 µL of the two phases in a 5 mL vial made of Teflon. The phases were highly stirred during 1 to 4 hours. After centrifugation, aliquots of the two phases (350 µL) were separated and their activities were measured using a gamma counter (Packard Cobra II Auto Gamma).

This project has received funding from the EURATOM research and training programme 2014-2018 under grant agreement No 755171. The content of this deliverable reflects only the author's view. The European Commission is not responsible for any use that may be made of the information it contains.

In this study, 2 types of membranes purchased from Merck Millipore were employed. For aqueous solutions: the hydrophilic Omnipore PTFE membrane (JHWP04700, pore size 0.45 µm, porosity of 80%); for organic solutions: the hydrophobic Durapore PVDF membrane (HVHP04700, pore size 0.45 µm, porosity of 75%). The membrane thickness, *L*, was measured: 58 µm for JHWP04700 and 102 µm for HVHP04700. These membranes were chosen because they are quite inert chemically.

In this work, liquid Kapton (a polyimide, synthesized in our lab) was used to glue the membrane. The lower part of the plastic cylinder was covered with Kapton in order to isolate its surface from the solutions (especially the organic ones). Kapton was chosen for its very low interactions with the chemical systems studied in this work.

The diffusion and extraction experiments were carried out in a thermostatted chamber in which the temperature was controlled to ±1°C.

2. MEASUREMENT OF THE TORTUOSITY OF THE MEMBRANES

The tortuosity of a membrane, θ, was obtained by first measuring the diffusion coefficients of the ions using the closed capillary technique. Then a diffusion experiment was carried out with the RMC technique by placing the same solution in A and B (except for the diffusing solute which is present in A only). The knowledge of *D* values from the previous capillary experiment allowed an adjustment of the tortuosity of the membrane used in the RMC experiment. This led to values of θ = 2.51 for the hydrophilic JHWP04700 membrane, and of θ = 1.94 for the hydrophobic HVHP04700 membrane.

These values of the tortuosity for the two membranes were used for the subsequent determination of diffusion coefficients and rate constants with the RMC technique.

3. DIFFUSION COEFFICIENTS OF EU(III) AND AM(III)

The measurement of a diffusion coefficient[4-6] with the RMC required 1 hour to a maximum (as compared to several days with the capillary technique), and a small consumption of solution (2-3 mL). Similar results for the *D* values were obtained by this method as compared to those from the closed capillary technique.

The diffusion coefficients of ^{241}Am(III) could not be determined by the capillary technique because ^{241}Am(III) is a γ-emitter of low energy, which would impose the use of high amounts of tracer. No data for the diffusion coefficient of Eu(III) and Am(III) in the literature were found for our extraction systems.

This project has received funding from the EURATOM research and training programme 2014-2018 under grant agreement No 755171. The content of this deliverable reflects only the author's view. The European Commission is not responsible for any use that may be made of the information it contains.

Table 1 collects the diffusion coefficients D(Eu) of radioactive ^{152}Eu(III) in aqueous solutions. It is observed that the RMC and the capillary technique give similar results for D(Eu), which indicates a good reliability of the RMC technique for the determination of the tortuosity of a membrane and of the diffusion coefficients. The hydrodynamic radii, r, of Eu(III) ion were computed from the value of D(Eu) by using the Stokes-Einstein equation,

$$r = k_B\, T/(6\pi\, \eta\, D) \qquad (6)$$

with k_B the Boltzmann constant, T the temperature, and η the dynamic viscosity of the solvent.

Table 5 : Diffusion coefficients (D) and hydrodynamic radii (r) of radioactive ^{152}Eu(III) in aqueous solutions.

Aqueous solution	Method	T (°C)	D(Eu) (cm^2/s)	r (Å)
0.5 M HNO_3	RMC	22	5.33×10^{-6}	4.32
	Capillary	22	5.72×10^{-6}	4.02
3 M HNO_3	RMC	22	4.54×10^{-6}	4.85
10 mM SO_3-Ph-BTP in 0.5M HNO_3	RMC	22	3.66×10^{-6}	6.31
	Capillary	22	3.63×10^{-6}	6.35
20 mM SO_3-Ph-BTP in 0.5M HNO_3	RMC	22	3.13×10^{-6}	7.06
	Capillary	22	3.03×10^{-6}	7.37
	RMC	35	3.84×10^{-6}	7.99
40 mM SO_3-Ph-BTP in 0.5M HNO_3	Capillary	22	2.67×10^{-6}	7.71
40 mM PTD in 0.5M HNO_3	RMC	22	3.17×10^{-6}	6.92
80 mM PTD in 0.5M HNO_3	RMC	22	3.04×10^{-6}	7.19
100 mM PTD in 0.5M HNO_3	RMC	22	2.86×10^{-6}	7.73

The radius r provides interesting information about the size of the complex in solution. In a nitrate solution, the mono-nitrate and bis-nitrate complexes of Eu(III) are characterized by low complexation constants (K_1 = 6.50 and K_2 = 1.97 at 20°C[7,8]) and thus, an hydrated Eu(III) ion is expected to be the dominant species in dilute 0.5 M HNO_3. D and r values for Eu(III) obtained in 0.5 M HNO_3 are comparable to the results reported in 1 M $HClO_4$ solution[3] (D(Eu) = 5.7×10^{-6} (cm^2/s) and r = 4.1 Å), in which the Eu(III) ions were aqua-ions; they were not complexed because the perchlorate anion is a very weak complexing ligand[9,10,11]. In concentrated 3 M HNO_3 where the mono- and bis-nitrate complexes are formed in appreciable amounts, the D value is significantly smaller, and the radius r=4.85 Å is larger, than in 0.5 M HNO_3, as could be expected because the Eu(III) ion is more complexed by nitrates in 3 M HNO_3[12,13]. However, the difference is not large.

This project has received funding from the EURATOM research and training programme 2014-2018 under grant agreement No 755171. The content of this deliverable reflects only the author's view. The European Commission is not responsible for any use that may be made of the information it contains.

In the case of the bulky SO_3-Ph-BTP ligand in aqueous solution, the Eu–SO_3-Ph-BTP complex was likely to be formed in appreciable amount[14], which resulted in a lower *D*(Eu) and a greater radius *r*. For Eu(III) in 20 mM SO_3-Ph-BTP solution, *D*(Eu) increased when *T* was changed from 22°C to 35°C, but the radius *r* was unchanged because of the increase of *T* and the decrease of the viscosity (see Eq. 6).

The diffusion coefficients of ^{152}Eu(III) in different organic solutions are collected in Table 2. Similar results were also obtained here when using the RMC and capillary techniques, which is a satisfying result. Diffusion was found slower in organic solutions than in aqueous. The *D* values were significantly low in viscous 1-octanol. In the presence of bulky ligands such as TODGA and $CyMe_4$-BTBP in solutions pre-equilibrated with nitric acid solution, where Eu(III)–ligand–NO_3^- complexes are dominantly formed [16-23], the *r* values of 6-9 (Å) are close to those obtained for aqueous SO_3-Ph-BTP complexes. In TPH, loading of HNO_3 in organic phase (by equilibrating it with aqueous 0.5M or 3M nitric acid), did not influence *D*(Eu) and *r*. Similarly, varying the concentration of TODGA in the range 0-5 mM and that of $CyMe_4$-BTBP (0-10 mM) in 1-octanol resulted in comparable values of *D*(Eu) and *r*.

Table 6 : Diffusion coefficients (*D*) and hydrodynamic radii (*r*) of radioactive ^{152}Eu(III) in organic solutions.

Organic solution	Method	*T* (°C)	*D*(Eu) (cm^2/s)	*r* (Å)
0.2M TODGA + 5%vol. 1-octanol in TPH (equilibrated with 0.5M HNO_3)	Capillary	22	1.21×10^{-6}	8.71
	RMC	35	1.82×10^{-6}	7.71
0.2M TODGA + 5%vol. 1-octanol in TPH (equilibrated with 3M HNO_3)	RMC	22	1.22×10^{-6}	8.41
5mM TODGA in 1-octanol (equilibrated with 3M HNO_3)	RMC	22	3.92×10^{-7}	6.35
	Capillary	22	3.96×10^{-7}	6.30
10mM $CyMe_4$-BTBP in 1-octanol (equilibrated with 3M HNO_3)	RMC	22	4.02×10^{-7}	6.24
5mM $CyMe_4$-BTBP + 5mM TODGA in 1- octanol (equilibrated with 3M HNO_3)	RMC	22	4.03×10^{-7}	6.35
10mM $CyMe_4$-BTBP + 5mM TODGA in 1-octanol (equilibrated with 3M HNO_3)	RMC	22	3.93×10^{-7}	6.35
	Capillary	22	3.83×10^{-7}	6.52
	RMC	35	6.97×10^{-7}	6.17

This project has received funding from the EURATOM research and training programme 2014-2018 under grant agreement No 755171. The content of this deliverable reflects only the author's view. The European Commission is not responsible for any use that may be made of the information it contains.

The diffusion coefficients of radioactive ^{241}Am(III) in aqueous and organic solutions determined with the RMC technique are recapitulated in Table 3. It can be seen that, in the same experimental conditions (composition of solutions, temperature), the experimental results for Am(III) and Eu(III) point to comparable values for *D* and *r*.

Table 7 : Diffusion coefficients (*D*) and hydrodynamic radii (*r*) of radioactive ^{241}Am(III) in aqueous and organic solutions.

	Method	*T* (°C)	*D*(Am) (cm^2/s)	*r* (Å)
Aqueous solution				
0.5 M HNO_3	RMC	22	5.54×10^{-6}	4.2
3 M HNO_3	RMC	22	4.94×10^{-6}	4.4
10 mM SO_3-Ph-BTP in 0.5M HNO_3	RMC	22	3.02×10^{-6}	7.7
20 mM SO_3-Ph-BTP in 0.5M HNO_3	RMC	22	2.92×10^{-6}	7.7
	RMC	35	3.75×10^{-6}	8.1
20 mM SO_3-Ph-BTP in 1M HNO_3	RMC	22	2.74×10^{-6}	8.0
20 mM SO_3-Ph-BTP in 2M HNO_3	RMC	22	2.73×10^{-6}	8.0
40 mM SO_3-Ph-BTP in 0.5M HNO_3	RMC	22	2.84×10^{-6}	7.4
40 mM PTD in 0.5M HNO_3	RMC	22	3.03×10^{-6}	7.5
80 mM PTD in 0.5M HNO_3	RMC	22	2.86×10^{-6}	7.9
100 mM PTD in 0.5M HNO_3	RMC	22	2.80×10^{-6}	8.1
Organic solution				
0.2M TODGA + 5%vol. 1-octanol in TPH (equilibrated with 0.5M HNO_3)	RMC	22	1.21×10^{-6}	9.09
	RMC	35	1.93×10^{-6}	8.51
0.2M TODGA + 5%vol. 1-octanol in TPH (equilibrated with 3M HNO_3)	RMC	22	1.21×10^{-6}	7.97
5 mM TODGA in 1-octanol (equilibrated with 3M HNO_3)	RMC	22	3.93×10^{-7}	6.36
10 mM $CyMe_4$-BTBP in 1-octanol (equilibrated with 3M HNO_3)	RMC	22	3.63×10^{-7}	6.85
5 mM $CyMe_4$-BTBP + 5 mM TODGA in 1-octanol (equilibrated with 3M HNO_3)	RMC	22	3.75×10^{-7}	6.71
10 mM $CyMe_4$-BTBP + 5mM TODGA in 1-octanol (equilibrated with 3M HNO_3)	RMC	35	6.95×10^{-7}	6.05
	RMC	22	3.62×10^{-7}	6.93

This project has received funding from the EURATOM research and training programme 2014-2018 under grant agreement No 755171. The content of this deliverable reflects only the author's view. The European Commission is not responsible for any use that may be made of the information it contains.

4. RESULTS: KINETICS OF EXTRACTION AND STRIPPING

The two phases were pre-equilibrated (except for the metal) by contacting them prior to all kinetic experiments.

1. VALIDATION OF THE TECHNIQUE

The rate constants k_f and k_r can be determined from extraction or stripping experiments with the RMC technique. The results obtained in the two ways should of course be identical.

Figure 2 and Table 4 show the results obtained for the system where the aqueous phase was composed of 20 mM SO_3-Ph-BTP and 0.5 M HNO_3, and the organic phase was 0.2M TODGA + 5% vol. 1-octanol in TPH. It can be seen in Table 4 that the rate constants k_f and k_r obtained in the two experimental configurations are comparable within experimental uncertainty which may be at least of the order of 20% in kinetic experiments. For this reason the results for the rate constant values will be given with 2 significant figures only.

It should be recalled that these experiments were carried out using two different types of membrane: the hydrophilic Omnipore JHWP membrane for extraction, and the hydrophobic HVHP membrane for stripping.

Let us note that the uncertainty is expected to be especially high in an extraction experiment when K is low or in a stripping experiment when K is high. In these cases indeed, even small deviations of the flow in the outer solution from the theoretical rotating disk hydrodynamics, may have a great effect on the rate of transfer.

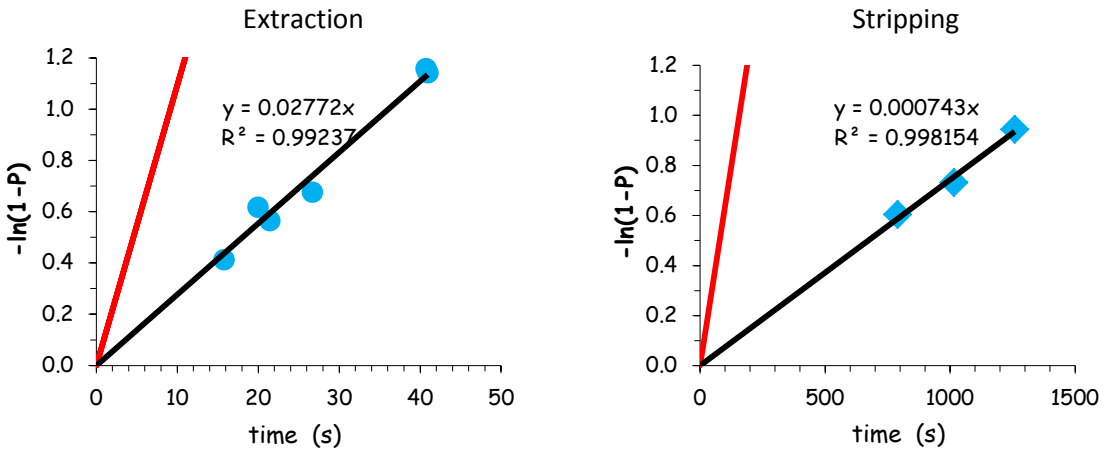

Figure 2 : Proportion of extracted Eu(III), *P*, as a function of time in the case of extraction (left) and stripping (right) experiments. Red line = diffusive limit (Eqs. 1 and 5). Organic phase: 0.2M TODGA (+5% vol. octanol-1) in TPH. Aqueous phase: 20 mM SO_3-Ph-BTP in 0.5M HNO_3. RMC at 600 rpm, T = 22 ± 1 °C.

This project has received funding from the EURATOM research and training programme 2014-2018 under grant agreement No 755171. The content of this deliverable reflects only the author's view. The European Commission is not responsible for any use that may be made of the information it contains.

Table 8 : Kinetic rate constants obtained from extraction and stripping experiments for the solutions of Figure 2.

	Distribution ratio, K	k_f (cm/s) aq → org	k_r (cm/s) org → aq
Extraction	30.6	2.2×10^{-4}	7.4×10^{-6}
Stripping		2.6×10^{-4}	8.6×10^{-6}

2. KINETICS WITH TODGA (+5% VOL. 1-OCTANOL)

2.1 EFFECT OF ROTATION SPEED

Figure 3 shows the influence of the rotation speed on the kinetics of stripping of Eu-152 from a 0.5M TODGA solution into 0.5M HNO_3. The rotation speed was expected to have an appreciable influence because the distribution ratio is high in this case (K = 329); therefore if the membrane contains the organic phase, the resistance in the external aqueous phase is large and strongly dependent on the rotation speed.

As expected, an increase of the rotation speed from 200 rpm to 600 rpm increased the rate of stripping, but the values of the extraction rate constants remained approximately constant: the aqueous-to-organic rate constant k_f was ≈ 1.9×10^{-3} cm/s at 200 rpm and ≈2.1×10^{-3} cm/s at 600 rpm, which values are within the experimental uncertainty.

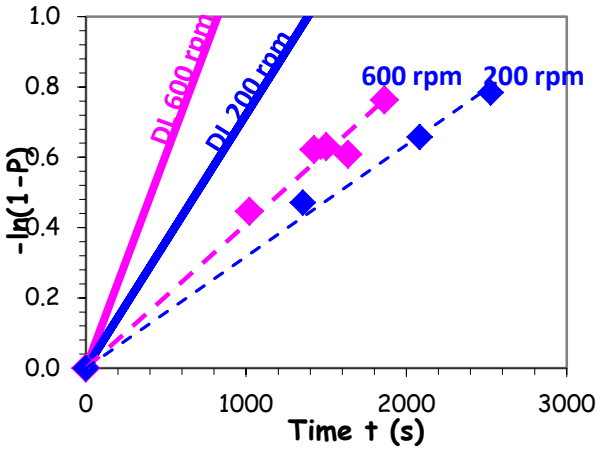

Figure 3: Influence of rotation speed on the rate of stripping of Eu-152. Organic phase: 0.2 M TODGA (+5% vol. 1-octanol) in TPH. Aqueous phase: 0.5 M HNO_3. T = 22 ± 1 °C. DL represents the theoretical diffusive limit (for infinitely fast kinetics).

This project has received funding from the EURATOM research and training programme 2014-2018 under grant agreement No 755171. The content of this deliverable reflects only the author's view. The European Commission is not responsible for any use that may be made of the information it contains.

This is a satisfactory result since the discrepancy between the two values is ≈10%, which is low in view of the fact that the kinetics are rather fast in this case.

A similar effect of the rotation speed on the kinetics was also found in the case of the stripping of Am-241 from a TODGA solution, as shown in Figure 4. The rate constant k_f is nearly constant, with values of 3.2×10^{-3} cm/s at 200 rpm and 3.5×10^{-3} cm/s at 600 rpm (≈ a 10% discrepancy also in this case).

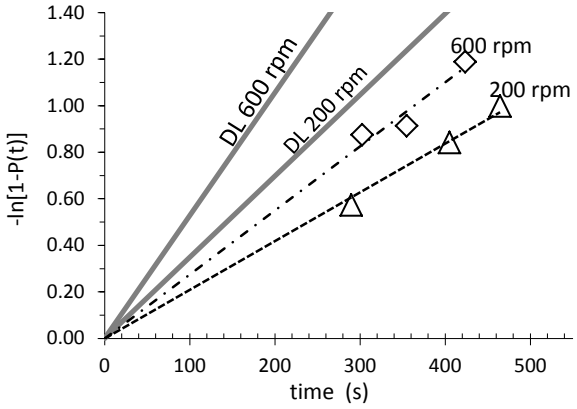

Figure 4: Influence of the rotation speed on the stripping rate of Am-241. Organic phase: 0.2M TODGA (+5% vol. 1-octanol) in TPH. Aqueous phase: 0.5M HNO_3. *T* = 22 ± 1 °C. DL = theoretical diffusive limit (for infinitely fast kinetics).

2.2. EFFECT OF HNO_3 CONCENTRATION

^{152}Eu(III) and ^{241}Am(III) were separately extracted from 0.5M and 3M HNO_3 solutions into 0.2M TODGA +5% vol. 1-octanol in TPH. The results for the extraction kinetics are collected in Table 5.

Table 9 : Extraction kinetics of ^{152}Eu(III) and ^{241}Am(III) by 0.2 M TODGA + 5% vol. 1-octanol in TPH from aqueous solutions of different concentrations [HNO_3]. RMC technique used at rotation speed = 600 rpm, *T* = 22 ± 1 °C.

Cations	Aqueous	*K*	k_f (cm/s) aq → org	k_r (cm/s) org → aq
$^{152}Eu^{3+}$	0.5 M HNO_3	329	2.4×10^{-3}	6.9×10^{-6}
	3 M HNO_3	1044	3.1×10^{-3}	3.0×10^{-6}
$^{241}Am^{3+}$	0.5 M HNO_3	58	2.8×10^{-3}	4.8×10^{-6}
	3 M HNO_3	2977	3.9×10^{-3}	1.3×10^{-6}

This project has received funding from the EURATOM research and training programme 2014-2018 under grant agreement No 755171. The content of this deliverable reflects only the author's view. The European Commission is not responsible for any use that may be made of the information it contains.

The distribution ratios *K* for Eu(III) and Am(III) are strongly enhanced when [HNO_3] is varied from 0.5M to 3M, as expected from Le Chatelier principle for the extraction reaction by TODGA from nitric acid solution[24,25,26],

$$M^{n+}_{aq.} + nNO^{-}_{3aq.} + mL_{org.} \overset{K_{ex}}{\rightleftharpoons} M(NO_3)_n \cdot mL_{org.}$$

The extraction rates k_f of Eu(III) and Am(III) are found to be of comparable high magnitudes, and they increase with [HNO_3] by about 30%. The kinetics are quite fast with k_f values of a few 10^{-3} cm/s. On the other hand, the stripping of these cations from TODGA solution to aqueous nitric acid was slow with k_r values of the order of a few 10^{-6} cm/s. The stripping rate constants drop by ≈60% and 70% in the case of Eu(III) and Am(III), respectively.

2.3. EFFECT OF TODGA CONCENTRATION

The influence of TODGA concentration on the kinetics of extraction of Eu-152 was investigated. As shown in Figure 5, when the TODGA concentration was increased from 0.1 M to 0.4 M, the distribution ratio *K* highly enhanced, showing strong complexation of TODGA.

The stripping rate (org-to-aq k_r) was considerably slower when $[TODGA]_{org}$ was increased. At the same time, the extraction rate (aq-to-org k_f) dropped a little.

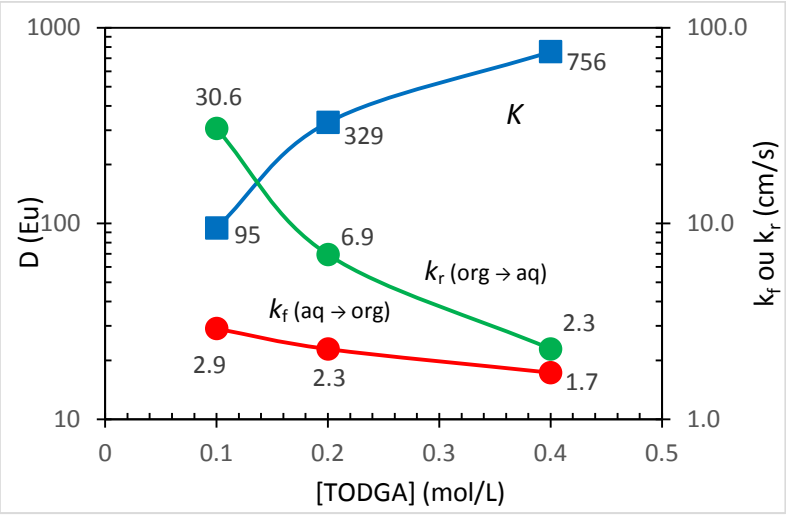

Figure 5 : Distribution ratio *K* (■), and extraction (k_f, ●, in units of 10^{-3} cm/s) and stripping (k_r, ●, in units of 10^{-6} cm/s) rate constants in the case of ^{152}Eu(III). Organic phase: TODGA (+5% vol. 1-octanol) in TPH. Aqueous phase: 0.5 M HNO_3. RMC technique with rotation speed = 600 rpm, *T* = 22 ± 1 °C.

This project has received funding from the EURATOM research and training programme 2014-2018 under grant agreement No 755171. The content of this deliverable reflects only the author's view. The European Commission is not responsible for any use that may be made of the information it contains.

In a previous HYPAR report we made the conjecture that the slowdown of the extraction rate might be due to the fact that the TODGA concentration at the interface increased with that in the bulk, thus causing a "congestion effect" at the interface becoming more "crowded" with extractant molecules. This interpretation rested on the finding that TODGA is surface active when it is dissolved in TPH as shown in Figure 6 (left). The same result was found by Nave et al.[27] in 2004 (see Figure 6, right), and with 2 M HNO_3 in aqueous phase.

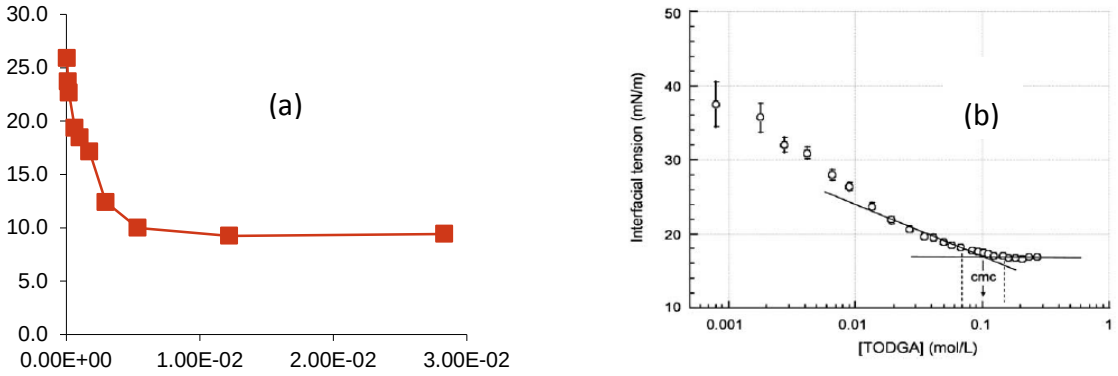

Figure 6: (a) Interfacial tension at the TPH+TODGA/water+3M HNO_3 interface vs. TODGA concentration at 22°C (measurement performed in ACSEPT in 2010); (b) Same type of measurement for the interface *n*-dodecane+TODGA/water+2M HNO3 at 25°C (taken from ref. 27).

However we have realized recently that this view is certainly incorrect because TODGA is *not* surface active in the system studied here. This was found by performing interfacial tension measurements, the result of which is shown in Figure 7. This is a surprising result, which might be due to the presence of 1-octanol in the organic phase (TPH instead of n-dodecane seem unlikely to explain the phenomenon). Besides, it was found that TODGA is not surface active when it is dissolved in 1-octanol (not shown)

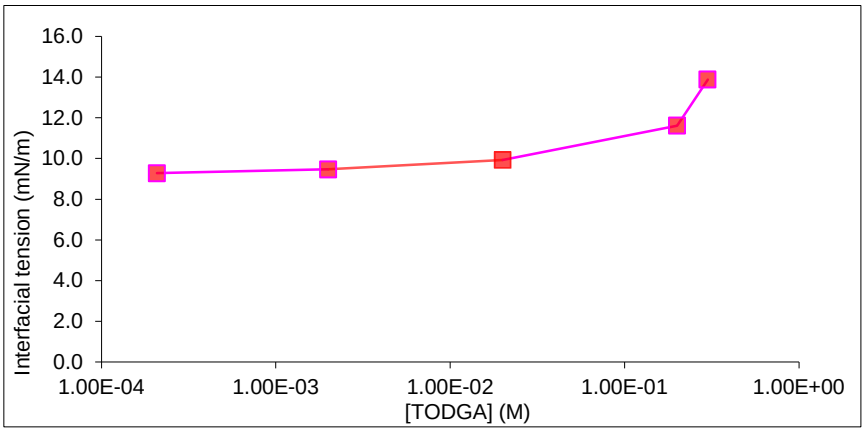

Figure 7: Interfacial tension of the interface between a 3 M HNO_3 solution and TODGA (+5% vol. 1-octanol) in TPH at 22°C as a function of the TODGA concentration in the range 2 x 10^{-4} M to 0.3 M.

This project has received funding from the EURATOM research and training programme 2014-2018 under grant agreement No 755171. The content of this deliverable reflects only the author's view. The European Commission is not responsible for any use that may be made of the information it contains.

Consequently, the slowdown observed in Figure 5 is counterintuitive, and not easy to interpret. In particular the slowdown of the extraction kinetics is quite surprising, even if it is moderate. One may indeed expect the probability of encounter between an Eu(III) ion and a TODGA molecule at the interface to be higher when more TODGA molecules are present in the organic phase (and thus expectedly in the vicinity of the interface), which would make the transfer faster. But this is not the case. An explanation for this phenomenon therefore remains to be found.

2.4. EXTRACTION OF HNO_3

In SACSESS, it had been noticed that, in scrubbing conditions, the co-extraction of HNO_3 accelerated the extraction of Eu(III) by TODGA/1-octanol system (see Deliverable D12.5, SACSESS 2015). It appeared therefore instructive to study also the extraction of HNO_3 by TODGA (+ 1-octanol).

Figure 8 shows the extraction rate of nitric acid, and of Eu(III) for comparison. The two processes have a linear behavior when -ln[1-P(t)] is plotted as a function of time.

The use of Eq. 1 ($-\ln[1-P(t)] = t / \tau$) leads to a value of 20.2 s for the mean-passage time τ for Eu(III) (from 3M HNO_3 into *pre-equilibrated* organic solution), and of 75.2 s for the transfer of HNO_3 (from 3M HNO_3 into fresh solvent).

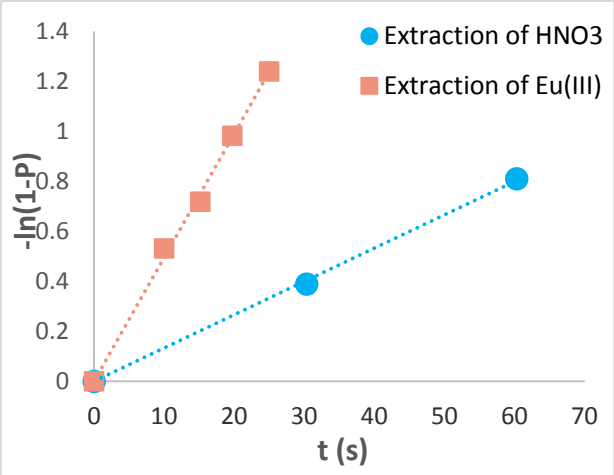

Figure 8: Extraction kinetics of HNO_3 by TODGA solution (●) compared with that of Eu(III) (■). Organic phase: TODGA (+5% vol. 1-octanol) in TPH. Aqueous phase: 3 M HNO_3 (in the hydrophilic HVLP membrane). RMC technique with rotation speed = 600 rpm, *T* = 22 ± 1 °C.

This project has received funding from the EURATOM research and training programme 2014-2018 under grant agreement No 755171. The content of this deliverable reflects only the author's view. The European Commission is not responsible for any use that may be made of the information it contains.

It is seen on this figure that the transfer of HNO_3 is significantly slower than that of Eu(III). A first analysis of the rate data shows that the extraction kinetics of HNO_3 is appreciably slower than that of Eu(III), of the order of 4 times slower. However an estimation of the kinetic rate parameters for nitric acid will require a more refined analysis of the diffusion rates in each phase.

3. KINETICS OF STRIPPING

Eu(III) and Am(III) were co-extracted in organic TODGA solution and then separated by selective stripping of Am(III) into aqueous solution by using a stripping ligand. The promising aqueous stripping ligands for *i*-SANEX and GANEX processes, SO_3-Ph-BTP[27] and PTD[29, 34], were used in this study.

3.1 ADDITION OF SO_3-PH-BTP

3.1.1 EFFECT OF SO_3-PH-BTP CONCENTRATION

Figure 9 shows the results for the stripping of Eu(III) (Fig. 9a) and of Am(III) (Fig. 9b) from organic TODGA solution into aqueous 0.5 M HNO_3 solutions with different concentrations of $[SO_3\text{-Ph-BTP}]_{aq}$ from 10 mM to 40 mM. The rate constant k_f in Figure 9 is for aqueous-to-organic transfer of the solute (extraction) and k_r is for organic-to-aqueous transfer (stripping).

As expected an increase of $[SO_3\text{-Ph-BTP}]_{aq}$ strongly decreased the distribution ratio *K* of Eu(III) and Am(III). The dependencies are approximately linear in log-log scale with a slope close to -1.7 for both Eu-152 and Am-241. The separation factors $SF = K(Eu)/K(Am)$ were high (between 727 at 10mM SO_3-Ph-BTP and 660 at 40mM SO_3-Ph-BTP), which shows the actinide-selective stripping by the aqueous ligand.

The extraction rates were moderate and considerably slower for both Eu-152 and Am-241 when $[SO_3\text{-Ph-BTP}]_{aq}$ was increased. The dependencies are linear with a slope of -1.0 for Eu-152 and -0.9 for Am-241 in a log-log plot. For any $[SO_3\text{-Ph-BTP}]_{aq}$, the extraction rate constant k_f for Eu-152 is observed to be about 10 times higher than that for Am-241.

The stripping rates for both Eu-152 and Am-241 were faster by addition of SO_3-Ph-BTP. This may be interpreted by the fact that the cations at the interface have a higher probability of reacting with a ligand SO_3-Ph-BTP molecule coming from the bulk aqueous phase. The enhancement of the stripping rate was similar for Eu-152 and Am-241, with slopes of about

This project has received funding from the EURATOM research and training programme 2014-2018 under grant agreement No 755171. The content of this deliverable reflects only the author's view. The European Commission is not responsible for any use that may be made of the information it contains.

0.7 of the dependencies in log-log scale. Moreover, with k_r values of Am-241 on the order of 10^{-4} – 10^{-3} (cm/s), the stripping rate for Am-241 was rather fast, and greatly faster than that for Eu-152. The ratio of the stripping rate constants, k_r(Am)/k_r(Eu), varied from 63 (at 10 mM SO_3-Ph-BTP) to 118 (at 40 mM SO_3-Ph-BTP).

As a result, the separation of Am(III) over Eu(III) by stripping with SO_3-Ph-BTP is greatly favored both thermodynamically and kinetically.

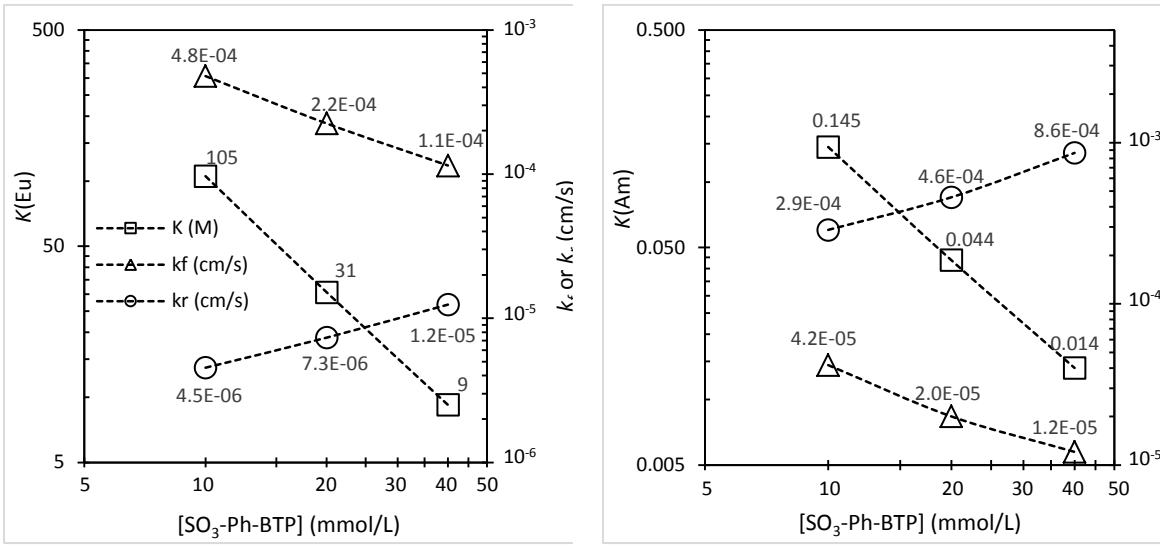

Figure 8 : Extraction and stripping kinetic rate constants, and *K* values, for ^{152}Eu(III) (a) and ^{241}Am(III) (b) in the case of aqueous 0.5 M HNO_3 solutions of different $[SO_3\text{-Ph-BTP}]_{aq}$ concentrations and 0.2 M TODGA (+5% vol. 1-octanol) in TPH. RMC at rotation speed = 600 rpm, *T* = 22.5 ± 1 °C.

3.1.2 EFFECT OF HNO_3 CONCENTRATION

As discussed in SACSESS HYBAR1 report from KIT, to avoid sulfur-containing wastes being produced from destroying SO_3-Ph-BTP in the downstream of GANEX and *i*-SANEX processes, actinides should be separated from SO_3-Ph-BTP, allowing for recycling of the latter. So, actinides could be re-extracted from aqueous SO_3-Ph-BTP into organic TODGA solution by increasing the TODGA concentration and/or that of HNO_3. Re-extraction using higher HNO_3 concentration was proposed to be preferable in SACSESS HYBAR2 KIT report.

In this study, following the conclusion of this report, the kinetics of re-extraction of Am(III) was studied by increasing $[HNO_3]_{aq}$ from 0.5 M to 2 M. In Figure 10 are plotted the results of

This project has received funding from the EURATOM research and training programme 2014-2018 under grant agreement No 755171. The content of this deliverable reflects only the author's view. The European Commission is not responsible for any use that may be made of the information it contains.

the extraction of Am(III) by 0.2 M TODGA solution from aqueous 20 mM SO_3-Ph-BTP with various HNO_3 concentrations.

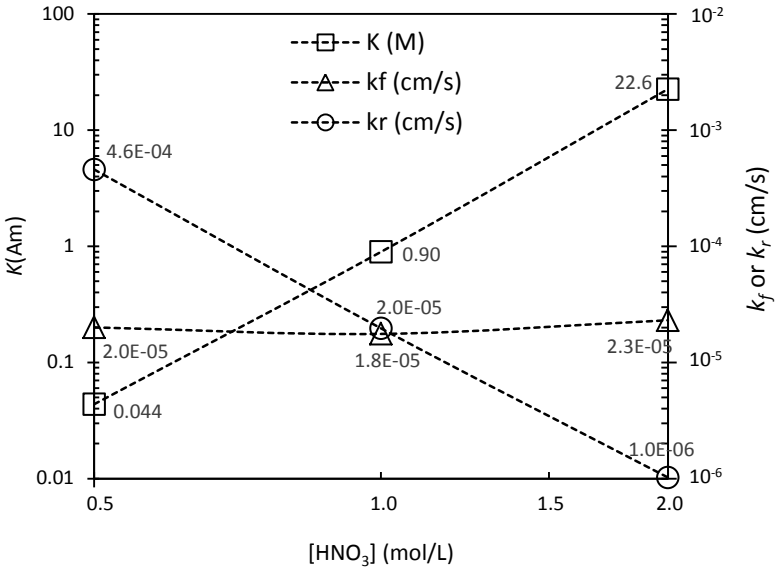

Figure 9: Re-extraction and stripping rates, and *K* values, for ^{241}Am(III) between aqueous 20mM SO_3-Ph-BTP solutions of different HNO_3 concentrations and organic 0.2M TODGA (+5% vol. 1-octanol) in TPH (RMC at rotation speed = 600 rpm, *T* = 22.5 ± 1 °C).

The SO_3-Ph-BTP ligand possesses a known monoprotonation constant value, pK_{HBTP} = 0.5 - 0.6 [30,31]. The H.SO_3-Ph-BTP, monoprotonated on a donor N atom of the central pyridine moiety, does not complex the Am(III) ions[31]. As the acidity of the aqueous phase is increased, more ligand becomes (mono-)protonated, which decreases the amount of free ligand available to strip Am(III). This was confirmed in our experiments, as shown in Figure 10. Increasing [HNO_3] from 0.5 M to 2 M slowed down considerably the stripping rate from k_r = 4.6 x 10^{-4} cm/s to 1.0 x 10^{-6} cm/s, and it increased the distribution ratio *K*(Am). However, the variation of $[HNO_3]_{aq}$ did not modify the re-extraction kinetics, for which the rate constant k_f remained constant (see Figure 10). The rates k_f of about 2.0 x 10^{-5} (cm/s) are of moderate value.

3.2 PTD

The disadvantage of SO_3-Ph-BTP ligand is that it does not comply with the CHON principle for complete incineration. The PTD ligand, which satisfies the CHON principle, has shown a good alternative for stripping actinides from organic solutions[29,33]. It was used in this work.

This project has received funding from the EURATOM research and training programme 2014-2018 under grant agreement No 755171. The content of this deliverable reflects only the author's view. The European Commission is not responsible for any use that may be made of the information it contains.

3.2.1 EFFECT OF PTD CONCENTRATION

The results for the distribution ratio, and the stripping and extraction rate constants, for 0.5 M HNO_3 and 0.2 M TODGA are collected in Table 6, and shown in Figures 11 and 12.

Table 6: Extraction kinetics of ^{152}Eu(III) and ^{241}Am(III) by 0.2 M TODGA + 5% vol. 1-octanol in TPH from aqueous solutions with [HNO_3] = 0.5 M. RMC technique used at rotation speed = 600 rpm, T = 22 ± 1 °C.

Cation	[PTD]	K	k_f (cm/s) aq → org	k_r (cm/s) org → aq
$^{152}Eu^{3+}$	40 mM	155	2.6×10^{-3}	1.7×10^{-5}
	80 mM	99	2.2×10^{-3}	2.3×10^{-5}
	100 mM	90	1.8×10^{-3}	2.5×10^{-5}
$^{241}Am^{3+}$	40 mM	0.969	9.2×10^{-4}	9.6×10^{-4}
	80 mM	0.237	4.1×10^{-4}	17×10^{-4}
	100 mM	0.128	3.0×10^{-4}	23×10^{-4}

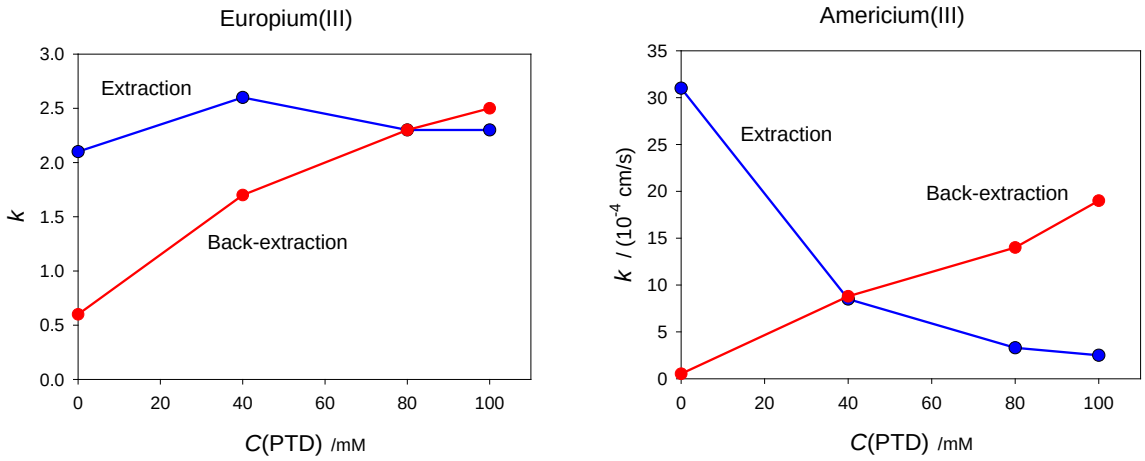

Figure 11: Extraction and stripping kinetic rate constants of ^{152}Eu(III) and ^{241}Am(III) as a function of added PTD concentration in aqueous phase (organic phase: 0.2 M TODGA (+5% vol. 1-octanol) in TPH). Plots for Eu(III) in units of 10^{-3} cm/s for k_{extr} and of 10^{-5} cm/s for k_{strip}. Plots for Am(III) in units of 10^{-4} cm/s.

It is seen in Table 6 that K decreases with [PTD] as expected. The extraction rate constant for Eu(III) is a few times larger than that for Am(III). On the other hand, the stripping rate constant for Eu(III) is about 2 orders of magnitude smaller than that for Am(III), but both increase significantly with [PTD].

This project has received funding from the EURATOM research and training programme 2014-2018 under grant agreement No 755171. The content of this deliverable reflects only the author's view. The European Commission is not responsible for any use that may be made of the information it contains.

Figure 11 shows that the extraction rate constant for Eu(III) is nearly constant with respect to the concentration of PTD. On the other hand it is observed that the rate constant for back-extraction increases with [PTD], which indicates that PTD captures the ion at the interface and accelerates its transfer relative to a PTD-free solution.

In Figure 11 we also see that the behavior of the extraction rate constant in the case of Am(III) is quite different from that of europium. Here the rate constant k_{extr} *decreases* sharply with the amount of added PTD, while it is nearly constant in the case of Eu(III) extraction. To the opposite, the rate constant for back-extraction, k_{strip}, increases notably with [PTD], with a 40 time increase from 0 to 100 mM of PTD. Here too, this suggests that PTD captures the ion at the interface; it accelerates its transfer to the aqueous phase, and it tends to retard its extraction to the organic phase.

3.2.2 EFFECT OF HNO_3 CONCENTRATION IN THE PRESENCE OF PTD

Here the study was done only in the case of Am(III) (because of a lack of time), for [PTD] = 80 mM and 0.2 M TODGA, for 2 values of [HNO_3] = 0.1 M and 0.5 M.

Table 7: Distribution ratio, *K*, and extraction kinetics of ^{241}Am(III) by 0.2 M TODGA + 5% vol. 1-octanol in TPH from aqueous solutions with [PTD] = 80 mM. RMC technique used at rotation speed = 600 rpm, *T* = 22 ± 1 °C.

Cation	[HNO_3]	*K*	k_f (cm/s) aq → org	k_r (cm/s) org → aq
$^{241}Am^{3+}$	0.1 M	1.05×10^{-3}	1.9×10^{-7}	1.8×10^{-4}
	0.5 M	0.237	4.1×10^{-4}	1.7×10^{-3}

In this table we see that *K* strongly increases with [HNO_3] from 0.1 M to 0.5 M. The extraction kinetics is greatly enhanced by more than 3 orders of magnitude, and the stripping kinetics is enhanced by about 10 times.

This project has received funding from the EURATOM research and training programme 2014-2018 under grant agreement No 755171. The content of this deliverable reflects only the author's view. The European Commission is not responsible for any use that may be made of the information it contains.

4. SELECTIVE EXTRACTION WITH CYME$_4$-BTBP (+ TODGA)

4.1 INFLUENCE OF THE PHASE-TRANSFER CATALYST TODGA

The combination of 10mM CyMe$_4$-BTBP + 5mM TODGA extractant has been retained for actinides selective extraction in GANEX and 1c-SANEX processes. In this study, Eu(III) and Am(III) were separately extracted from aqueous 3 M HNO_3 solution into organic solutions of CyMe$_4$-BTBP + TODGA in 1-octanol. The phase-transfer catalyst, TODGA, was employed with the aim of accelerating the extraction kinetics. The results are shown in Figure 12.

The actinide-selective extractant CyMe$_4$-BTBP at 10 mM yielded a high separation factor SF(Am/Eu) of about 105 when it was used alone, but a very slow extraction rate, with k_f on the order of 10^{-7} – 10^{-6} cm/s. A faster, but still very slow, rate was obtained for Am(III), with k_f(Am) = 7.2 x 10^{-6} cm/s which is 24 times larger than that for Eu(III).

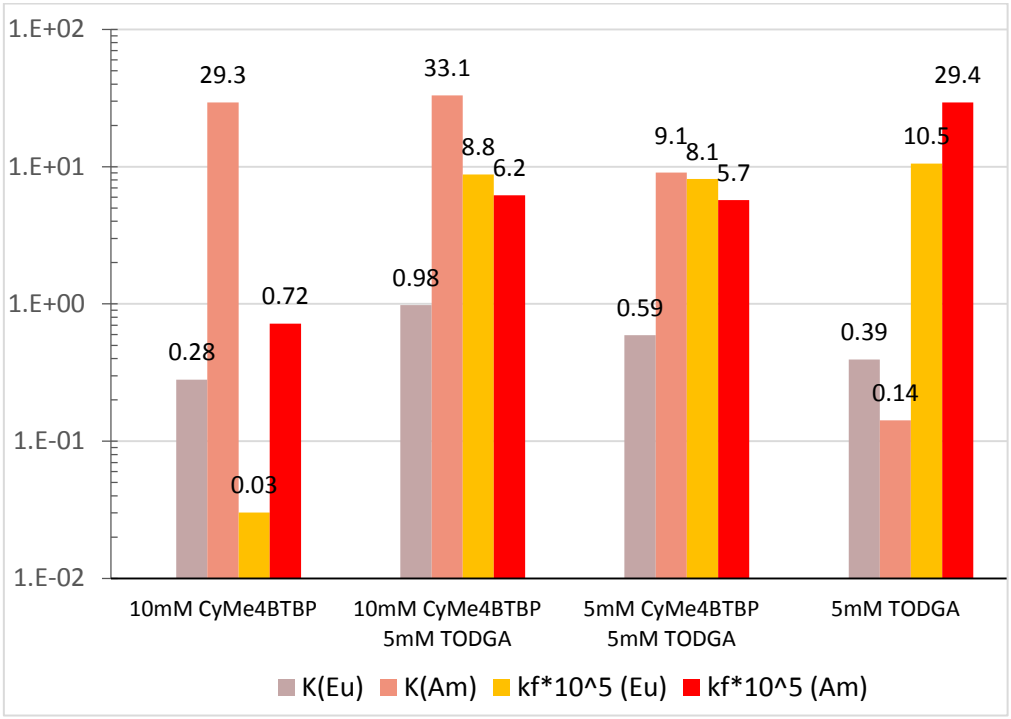

Figure 12: Effect of the phase-transfer catalyst TODGA on the kinetics of extraction by CyMe$_4$-BTBP. Aqueous phase: 3 M HNO_3 spiked with ^{152}Eu and/or ^{241}Am. Organic phase: 5 mM or 10 mM CyMe$_4$-BTBP with or without 5 mM TODGA in 1-octanol. RMC technique with rotation speed = 600 rpm, T = 22.5 ± 1 °C.

This project has received funding from the EURATOM research and training programme 2014-2018 under grant agreement No 755171. The content of this deliverable reflects only the author's view. The European Commission is not responsible for any use that may be made of the information it contains.

Fast extraction kinetics have been found above with TODGA alone. Even with a small amount of TODGA (5 mM) in TPH, a high rate constant was obtained for Am(III): k_f (Am) = 2.9 x 10^{-4} cm/s, which is 2.8 times greater than that for Eu(III): k_f (Eu) = 1.1 x 10^{-4} cm/s (see Figure 11, on the right). The distribution ratios *K*(Eu) and *K*(Am) were low.

A slight synergistic effect is observed in Figure 12, where the value of the distribution ratios *K* for the mixture 10 mM $CyMe_4$-BTBP + 5 mM TODGA are larger than the sum of the *K*'s for the individual extractants, for both Eu(III) (0.98 > 0.28+0.39 = 0.67) and Am(III) (33.1 > 29.3+0.14 = 29.4)extraction. Unfortunately, the separation factor is considerably reduced to SF(Am/Eu) = 34 as compared to that for $CyMe_4$-BTBP alone (SF = 105).

As regards the kinetics, it is clearly observed that the extraction kinetics of Eu(III) and Am(III) are greatly accelerated when the extractants are combined as compared to $CyMe_4$-BTBP alone: the rate constants k_f(Eu) and k_f(Am) are about 290 and 9 times higher, respectively. However, the rate k_f is of the order of a few 10^{-4} cm/s, which is a moderate value.

When [$CyMe_4$-BTBP] is lowered from 10 mM to 5 mM in the presence of 5 mM TODGA catalyst, the extraction kinetics of Eu(III) and Am(III) remain nearly unchanged (within the experimental uncertainty), although the distribution ratios are significantly lowered. This observation is consistent with the expectation that the kinetics are controlled by the TODGA, not by the $CyMe_4$-BTBP.

However it is also seen in Figure 12 that the rate constants for the mixture are lower than with TODGA alone (8.8 < 10.5 for k_f, and above all 6.2 << 29.4 for k_r).

4.2 EFFECT OF ADDED INACTIVE EU(III) IN MACRO-CONCENTRATION ON THE EXTRACTION KINETICS OF EU(III) AND AM(III)

In all the experiments presented above, we have used tracer amounts of ^{152}Eu or ^{241}Am. The kinetics of transfer of a solute is independent on its concentration as long as the latter is very low (e.g., of the order of 10^{-8} M or 10^{-6} M, expectedly).

In this section, we address the question of the influence of the solute concentration on the kinetics, a point that is seldom approached in the literature.

The extraction kinetics of traces of Eu-152 and of Am-241, from a 3 M HNO_3 solution to a 10 mM CyMe4BTBP (+5 mM TODGA) in 1-octanol, were studied in the presence of macro-concentrations of inactive Eu(III) in aqueous phase.

This project has received funding from the EURATOM research and training programme 2014-2018 under grant agreement No 755171. The content of this deliverable reflects only the author's view. The European Commission is not responsible for any use that may be made of the information it contains.

As could be expected it was found that the kinetics were slower when the concentration of Eu(III) was increased. This is shown in Figure 13 where the concentration of added Eu(III) goes from 0 to 0.1 M.

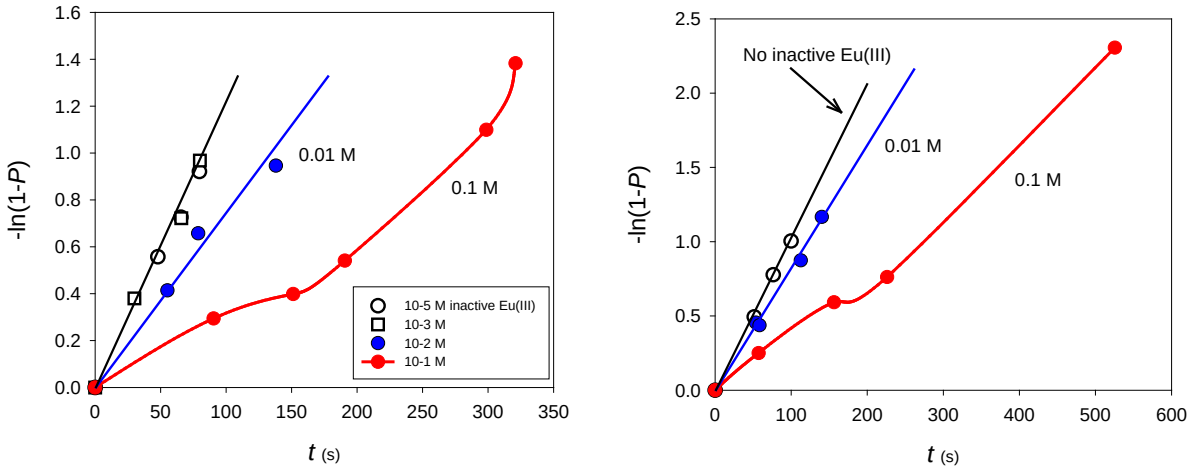

Figure 13: Extraction rate of traces of ^{152}Eu(III) (left) and of ^{241}Am(III) (right) as a function of time for various concentrations of added inactive Eu(III) (varying from 10^{-5} M to 0.1 M). Aqueous phase: 3 M HNO_3 solution; organic: 10 mM $CyMe_4BTBP$ + 5 mM TODGA in 1-octanol.

As noticed in this figure, when the amount of inactive Eu(III) exceeds some critical value - which seems to lie somewhere between 10^{-3} M and 0.01 M - the plot of –ln(1-*P(t)*) vs. time begins to drop, that is the relative extraction rate *P* starts to decrease. When the concentration of added Eu(III) is still more increased, –ln(1-*P(t)*) exhibits a peculiar non-linear behavior vs. time. This is due to the fact that the interfacial kinetic rate constant is no longer a constant in time, because it is a (decreasing) function of Eu(III) concentration in the vicinity of the interface, and this concentration decreases in time. When this concentration is high the ability of the organic phase to transfer the ion out of the aqueous phase drops, there is not enough extractant to capture the europium arriving at the interface with the same efficiency as when the concentration of europium is low. When the concentration of solute near the interface (on the aqueous side) increases above some critical value, the interface becomes too "crowded", the ions have to compete with other ions in order to find extractant molecules with which to react and be extracted. In that case, extractant molecules need be transported to the interfacial region where their concentration is depleted because of the extraction of solute ions; this transport may contribute significantly to the overall kinetics, as it does in the MTWCR model.

The case of americium ion is similar to that of europium. The rate is slowed down by the addition of inactive Eu(III). The kinetic rate constant is not a constant during the transfer of

This project has received funding from the EURATOM research and training programme 2014-2018 under grant agreement No 755171. The content of this deliverable reflects only the author's view. The European Commission is not responsible for any use that may be made of the information it contains.

Am(III). It starts to drop when the concentration of added inactive Eu(III) reaches a critical value somewhere between 10^{-3} M and 0.01 M.

4.3 EFFECT OF TEMPERATURE ON EXTRACTION KINETICS

The influence of the temperature on the kinetics of extraction has been examined at 2 temperatures of 25°C and 35°C. The results for the extraction of Eu(III) and Am(III) by 10 mM $CyMe_4$-BTBP + 5 mM TODGA in 1-octanol are collected in Table 8.

Table 8: Influence of temperature on extraction kinetics. Aqueous phase: 3M HNO_3 + ^{152}Eu or ^{241}Am. Organic phase: 10 mM $CyMe_4$-BTBP + 5 mM TODGA in 1-octanol. RMC technique with rotation speed = 600 rpm.

Radioelement	*T*	*K*	k_f (aq->org) (cm/s)
^{152}Eu	22°C	0.98	8.8 (± 1.2) x 10^{-5}
	35°C	0.67	6.1 (± 0.9) x 10^{-5}
^{241}Am	22°C	31.3	6.2 (± 0.3) x 10^{-5}
	35°C	22.4	5.6 (± 0.9) x 10^{-5}

An increase of the temperature from 22°C to 35°C lowers the distribution ratios *K*(Eu) and *K*(Am), indicating that the extraction reaction for both cations is exothermic. The values of *K*(Eu or Am) at 35°C are about 30% less than those at 22°C.

The extraction kinetics of Eu(III) seem to be slightly decelerated when the temperature is increased from 20°C to 35°C. Somewhat in contrast, they do not exhibit a clear trend in this temperature range in the case of Am(III). Indeed although one observes a small reduction in the rate constants k_f(Am), this variation is not very significant in view of the uncertainties on these values (see Table 8).

5. CONCLUSION

In this study two new types of membranes have been used. The aqueous/organic phases were placed in a hydrophilic/hydrophobic membrane, respectively. The results for the extraction and stripping kinetics were in agreement within the experimental uncertainty, which is of the order of 20%, or a bit more especially when the distribution ratio is very high

This project has received funding from the EURATOM research and training programme 2014-2018 under grant agreement No 755171. The content of this deliverable reflects only the author's view. The European Commission is not responsible for any use that may be made of the information it contains.

(higher uncertainty in the case of a stripping experiment) or very low (higher uncertainty in the case of an extraction experiment).

The values of the diffusion coefficients of the solutes Eu(III) and Am(III) in the phases, which are required in the treatment of the kinetic data, were measured using the RMC. The validity of the procedure was confirmed by separately measuring a few diffusion coefficients by using the closed capillary technique. The practical interest of employing the RMC for this purpose is that the measurement is obtained after a few minutes (instead of days with the capillary technique), and the *D* values are obtained with the same technique as for the kinetic measurements.

Extraction and stripping of Eu(III) and Am(III) have been studied for various concentrations of nitric acid and TODGA, possibly mixed with $CyMe_4$-BTBP, and also in the presence of the aqueous ligands SO_3-Ph-BTP and PTD.

It was somewhat striking to find that TODGA is not surface active at the interface between nitric acid and TODGA (+5% vol. of 1-octanol) in TPH. This contrasts with the case of TODGA in *n*-dodecane.

Another interesting result was the slowdown of the extraction rates of Eu(III) and Am(III) when the concentration of added Eu(III) is increased.

REFERENCES

1. J.P. Simonin, R. Mills, A. Perera, P. Turq, F. Tallet, *J. Solution Chem.,* 15(12), 1015-1030, 1986.
2. T. Rabockai and L. Jordan, Anal. Lett. 7, 647 (1974).
3. T. Rabockai, Electrochimica Acta, 1977, Vol. 22, 489-490
4. Heisel K. A., Goto J. J., Krishnan V. V., *Am. J. Anal. Chem.* 3, 401, 2012.
5. A.L. Rollet, J.P. Simonin, P. Turq, G. Gebel, R. Kahn, A. Vandais, J.P. Noel, C. Malveau, D. Canet, *J. Phys. Chem. B* 2001, 105*,* 4503-4509.
6. A.L. Rollet, J.P. Simonin, P. Turq, *Phys. Chem. Chem. Phys*., 2000, 2, 1029-1034.
7. H. B. Silber, F. Gaizer, T. Pham and M. Strozier,J. *Less Common Met., 126, 315* (1986).
8. H. B. Silber and *M. S. Strozier, Inorg. Chim. Acta,* 128, 267 (1987).
9. A. Baisden, G. R. Choppin, and W. F. Kinard, J. Inorg. Nucí. Chem., 34, 2029 (1972).
10. Y. Haas and G. Stein, *J. Phys. Chem*., 75, 3668 (1971).
11. P. J. Breen, W.D. Horrocks, *Inorg. Chem., 22, 536* (1983).
12. W.R. Fawcett, *Condensed Matter Phys*., 2005, 8, 2(42), 413–424.
13. H. D. B. Jenkins, and K. P. Thakur, *J. Chem. Educ.*, 1979, *56* (9), p 576
14. C.M. Ruff, U. Müllich, A. Geist and P.J. Panak, *Dalton Trans*., 2012, 41, 14594

This project has received funding from the EURATOM research and training programme 2014-2018 under grant agreement No 755171. The content of this deliverable reflects only the author's view. The European Commission is not responsible for any use that may be made of the information it contains.

15. L.G. Longsworth, Diffusion in Liquids and the Stokes-Einstein Relation, In T. Shedlovsky, Electro-chemistry in Biology and Medicine, p. 225. John Wiley, New York (1955).
16. Y. Sasaki, Y. Sugo, S. Suzuki and S. Tachimori, *Solvent Extr. Ion Exch*., 2001, 19, 91.
17. S. A. Ansari, P. N. Pathak, M. Husain, A. K. Prasad, V. S. Parmar and V. K. Manchanda, *Radiochim. Acta*, 2006, 94, 307.
18. Y. Sasaki, P. Rapold, M. Arisaka, M. Hirata, T. Kimura, C. Hill and G. Cote, *Solvent Extr. Ion Exch.*, 2007, 259, 187.
19. M. Arisaka and T. Kimura, *Solvent Extr. Ion Exch*., 2011, 29, 72.
20. C.Z. Wang, J.-H. Lan, Q.-Y. Wu, Y.-L. Zhao, X.-K. Wang, Z.-F. Chai and W.-Q. Shi, *Dalton Trans*., 2014, 43, 8713.
21. T.H. Vu, *Etude par spectrométrie de fluorescence de la solvatation et de la complexation des ions Eu(III) et Cm(III) en milieu octanol et à l'interface avec l'eau*. *Thèse de l'Université Louis Pasteur (Strasbourg)*, **2009**, Rapport CEA-R-6229.
22. A. Bremer, D.M. Whittaker, C.A. Sharrad, A. Geist, P.J. Panak, *Dalton Trans*., 2014, 43, 2684–2694.
23. P.J. Panak, A. Geist, *Chem. Rev.* 2013, 113, 1199−1236
24. Z. Wang, H. Huang, S. Ding, X. Hu, L. Zhang, Y. Liu, L. Song, Z. Chen, S. Li, *J. Radioanal. Nucl. Chem.*, 2017, 313(2), pp 309–318
25. Sasaki Y., Rapold P., Arisaka M., Hirata M., Kimura T., Hill C., Cote G., *Solvent Extr. Ion Exch.*, 2007, 25(2), 187–204.
26. S. A. Ansari, P.N. Pathak, M. Husain, A.K. Prasad, V. S. Parmar, V. K. Manchanda, *Radiochim. Acta*, 2006, 94, 307–312.
27. S. Nave, G. Modolo, C. Madic, F. Testard, Aggregation Properties of N,N,N',N'-Tetraoctyl-3-oxapentanediamide (TODGA) in n-Dodecane, Solvent Extr. Ion Exch., 22(4), 527, 2004.
28. Geist A., Müllich U., Magnusson D., Kaden P., Modolo, G., Wilden A., Zevaco T., Actinide(III)/Lanthanide(III) Separation Via Selective Aqueous Complexation of Actinides(III) using a Hydrophilic 2,6-Bis(1,2,4-Triazin-3-yl)-Pyridine in Nitric Acid. *Solvent Extr. Ion Exch.,* 2012, 30, 433−444.
29. E. Macerata, E. Mossini, S. Scaravaggi, M. Mariani, A. Mele, W. Panzeri, N. Boubals, L. Berthon, M.C. Charbonnel, F. Sansone, A. Arduini, and A. Casnati, *J. Am. Chem. Soc.,* 2016, 138, 7232−7235
30. C.M. Ruff, *Spektroskopische und thermodynamische Untersuchung der Komplexierung von Cm(III) und Eu(III) mit hydrophilen Bis-Triazinylpyridinen*; Dissertation, Universität Heidelberg, Germany, 2013.
31. Ł. Steczek, M. Rejnis, J. Narbutt, M.C. Charbonnel, P. Moisy, *J. Radioanal. Nucl. Chem.*, 2016, 309, 891–897.
32. J.E. Rodea, J. Narbutt, M.K. Dudek, S. Kaźmierski, J.C. Dobrowolski, *J. Mol. Liq*., 2016, 219, 224-231
33. E. Mossini , E. Macerata , A. Wilden , P. Kaufholzb, G. Modolo , N. Lotti, A. Casnati, A. Geist, and M. Mariani, *Solvent Extr. Ion Exch*., 2018, 36(4), 373–386.
34. C. Wagner, E. Mossini, E. Macerata, M. Mariani, A. Arduini, A. Casnati, A. Geist, and P.J. Panak, *Inorg. Chem.* 2017, 56, 2135−2144.

This project has received funding from the EURATOM research and training programme 2014-2018 under grant agreement No 755171. The content of this deliverable reflects only the author's view. The European Commission is not responsible for any use that may be made of the information it contains.

GENERAL CONCLUSION

Three types of experimental studies have been conducted in this project. The microfluidic cell technique implemented at CEA allows a direct contact of the phases. The other two (the RDC and the RMC) involve a membrane that is impregnated with one of the phases.

The RDC uses a version of the MTWCR model that leads to the determination of parameters such as the rate of transport of the extractant from the organic to aqueous phase, the rate of complexation and decomplexation of the metal with the ligand in the aqueous phase.

The microfluidic cell technique and the RMC aim at determining interfacial kinetic rate constants (the diffusion coefficients of the solute are determined in independent experiments).

Whilst slightly different techniques, the RDC and the RMC are still reporting similar rate constants when they look at similar systems. In the current report, that occurs in the RDC extraction experiments on the Ce(III)/TODGA system, and the RMC extraction experiments on the Eu(III) and Am(III)/TODGA system. ULANC reports an extraction rate constant of 6.6 µm/s for the Ce(III)/TODGA system (using 1M HNO3 in the aqueous phase), whilst CNRS-PHENIX reports analogous parameters of 24-31 and 28-39 µm/s for the Eu(III) and Am(III)/TODGA systems respectively (using acid in the range 0.5 to 3 M nitric). Agreement within a factor of 4 given the different trivalent cations used is rather satisfying.

Lastly it may be noticed that the kinetic rate constants used in process flowsheets (cf. the last meeting in Milan) are generally *global* kinetic rate constants that include the effect of transport in the diffusion layers adjacent to the aqueous/organic interfaces.

This project has received funding from the EURATOM research and training programme 2014-2018 under grant agreement No 755171. The content of this deliverable reflects only the author's view. The European Commission is not responsible for any use that may be made of the information it contains.